Geochemical study for dissolved methane in the high latitude ocean
～the Sea of Okhotsk and the Southern Ocean～

Osamu Yoshida

Table of Contents

Chapter 1　General Introduction

1.1　How much is the global warming?

The estimate of global surface temperature change is a 0.6℃ increase since the late 19th century with a 95% confidence interval of 0.4 to 0.8℃. The increase in temperature of 0.15℃ compared to that assessed in the IPCC WGI Second Assessment Report [*IPCC*, 1996] is partly due to the additional data for the last five years, together with improved methods of analysis and the fact that the SAR decided not to update the value in the First Assessment Report, despite slight additional warming. It is likely that there have been real differences between the rate of warming in the troposphere and the surface over the last twenty years, which are not fully understood. New palaeoclimate analyses for the last 1,000 years over the Northern Hemisphere indicate that the magnitude of 20th century warming is likely to have been the largest of any century during this period. In addition, the 1990s are likely to have been the warmest decade of the millennium. New analyses indicate that the global ocean has warmed significantly since the late 1940s: more than half of the increase in heat content has occurred in the upper 300 m, mainly since the late 1950s. The warming is superimposed on strong global decadal variability. Night minimum temperatures are continuing to increase, lengthening the freeze-free season in many mid- and high latitude regions. There has

been a reduction in the frequency of extreme low temperatures, without an equivalent increase in the frequency of extreme high temperatures. Over the last twenty-five years, it is likely that atmospheric water vapor has increased over the Northern Hemisphere in many regions. There has been quite a widespread reduction in daily and other sub-monthly time-scales of temperature variability during the 20th century. New evidence shows a decline in Arctic sea-ice extent, particularly in spring and summer. Consistent with this finding are analyses showing a near 40% decrease in the average thickness of summer Arctic sea ice over approximately the last thirty years, though uncertainties are difficult to estimate and the influence of multi-decadal variability cannot yet be assessed. Widespread increases are likely to have occurred in the proportion of total precipitation derived from heavy and extreme precipitation events over land in the mid- and high latitudes of the Northern Hemisphere.

1.2 Global methane budget

Methane (CH_4) is an atmospheric trace gas that contributes about 20% to the greenhouse effect, it is the second most in importance as a greenhouse gas after CO_2. Atmospheric levels of methane have varied by a factor of 2 and such variations have paralleled variation in global mean temperature over the same period.

Methane's globally averaged atmospheric surface abundance in 1998 was 1,745 ppb, corresponding to a total burden of about 4,850 Tg CH_4. The uncertainty in the burden is small ($\pm 5\%$) because the spatial and temporal distributions of tropospheric and stratospheric CH_4 have been determined by extensive high-precision measurements and the tropospheric variability is relatively small. For example, the Northern Hemisphere CH_4 abundances average about 5% higher than those in the Southern Hemisphere. Seasonal variations, with a minimum in late summer, are observed with peak-to-peak amplitudes of about 2% at mid-latitudes. The average vertical gradient in the troposphere is negligible, but CH_4 abundances in the stratosphere decrease rapidly

with altitude, e.g., to 1,400 ppb at 30 km altitude in the tropics and to 500 ppb at 30 km in high latitude northern winter.

The most important known sources of atmospheric methane are listed in *IPCC* [2001]. Although the major source terms of atmospheric methane have probably been identified, many of the source strengths are still uncertain due to the difficulty in assessing the global emission rates of the biospheric sources, whose strengths are highly variable in space and time: e.g., local emissions from most types of natural wetland can vary by a few orders of magnitude over a few meters. Nevertheless, new approaches have led to improved estimates of the global emissions rates from some source types. For instance, intensive studies on emissions from rice agriculture have substantially improved these emissions estimates [*Ding and Wang*, 1996; *Wang and Shangguan*, 1996]. Further, integration of emissions over a whole growth period (rather than looking at the emissions on individual days with different ambient temperatures) has lowered the estimates of CH_4 emissions from rice agriculture from about 80 Tg y^{-1} to about 40 Tg y^{-1} [*Neue and Sass*, 1998; *Sass et al.*, 1999]. There have also been attempts to deduce emission rates from observed spatial and temporal distributions of atmospheric methane through inverse modeling [e.g., *Hein et al.*, 1997; *Houweling et al.*, 1999]. The emissions so derived depend on the precise knowledge of the mean global loss rate and represent a relative attribution into aggregated sources of similar properties. The results of some of these studies have been included in *IPCC* [2001]. The global methane budget can also be constrained by measurements of stable isotopes ($\delta^{13}C$ and δD) and radiocarbon ($^{14}CH_4$) in atmospheric methane and in CH_4 from the major sources [e.g., *Stevens and Engelkemeir*, 1988; *Wahlen et al.*, 1989; *Quay et al.*, 1991, 1999; *Lassey et al.*, 1993; *Lowe et al.*, 1994]. So far the measurements of isotopic composition of CH_4 have served mainly to constrain the contribution from fossil fuel related sources. The emissions from the various sources sum up to a global total of about 600 Tg y^{-1}, of which about 60% are related to human activities such as

agriculture, fossil fuel use and waste disposal. This is consistent with the SRES estimate of 347 Tg y^{-1} for anthropogenic CH_4 emissions in the year 2000.

The current emissions from CH_4 hydrate deposits appear small, about 10 Tg y^{-1}. However, these deposits are enormous, about 107 Tg C [*Suess et al.*, 1999], and there is an indication of a catastrophic release of a gaseous carbon compound about 55 million years ago, which has been attributed to a large-scale perturbation of CH_4 hydrate deposits [*Dickens*, 1999; *Norris and Röhl*, 1999]. Recent research points to regional releases of CH_4 from clathrates in ocean sediments during the last 60,000 years [*Kennett et al.*, 2000], but much of this CH_4 is likely to be oxidized by bacteria before reaching the atmosphere [*Dickens*, 2001]. This evidence adds to the concern that the expected global warming may lead to an increase in these emissions and thus to another positive feedback in the climate system. So far, the size of that feedback has not been quantified. On the other hand, the historic record of atmospheric methane derived from ice cores [*Petit et al.*, 1999], which spans several large temperature swings plus glaciations, constrains the possible past releases from methane hydrates to the atmosphere. Indeed, *Brook et al.* [2000] find little evidence for rapid, massive CH_4 excursions that might be associated with large-scale decomposition of methane hydrates in sediments during the past 50,000 years.

The mean global loss rate of atmospheric methane is dominated by its reaction with OH in the troposphere.

$$OH + CH_4 \rightarrow CH_3 + H_2O$$
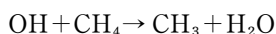
This loss term can be quantified with relatively good accuracy based on the mean global OH concentration derived from the methyl chloroform (CH_3CCl_3) budget described on OH. In that way we obtain a mean global loss rate of 507 Tg CH_4 y^{-1} for the current tropospheric removal of CH_4 by OH. In addition there are other minor removal processes for atmospheric CH_4. Reaction with Cl atoms in the marine boundary layer probably constitutes less than 2% of the total sink [*Singh et al.*, 1996]. A recent process model

study [*Ridgwell et al.*, 1999] suggested a soil sink of 38 Tg y^{-1}, and this can be compared to SAR estimates of 30 Tg y^{-1}. Minor amounts of CH_4 are also destroyed in the stratosphere by reactions with OH, Cl, and O(1D), resulting in a combined loss rate of 40 Tg y^{-1}. Summing these, the best estimate of the current global loss rate of atmospheric methane totals 576 Tg y^{-1}, which agrees reasonably with the total sources derived from process models. The atmospheric lifetime of CH_4 derived from this loss rate and the global burden is 8.4 years. Attributing individual lifetimes to the different components of CH_4 loss results in 9.6 years for loss due to tropospheric OH, 120 years for stratospheric loss, and 160 years for the soil sink (i.e., 1/8.4 y = 1/9.6 y + 1/120 y + 1/160 y).

The atmospheric abundance of CH_4 has increased by about a factor of 2.5 since the pre-industrial era as evidenced by measurements of CH_4 in air extracted from ice cores and firn [*Etheridge et al.*, 1998]. This increase still continues, albeit at a declining rate. The global tropospheric methane growth rate averaged over the period 1992 through 1998 is about 4.9 ppb y^{-1}, corresponding to an average annual increase in atmospheric burden of 14 Tg. Superimposed on this long-term decline in growth rate are interannual variations in the trend. There are no clear quantitative explanations for this variability, but understanding these variations in trend will ultimately help constrain specific budget terms. After the eruption of Mt. Pinatubo, a large positive anomaly in growth rate was observed at tropical latitudes. It has been attributed to short-term decreases in solar UV in the tropics immediately following the eruption that decreased OH formation rates in the troposphere [*Dlugokencky et al.*, 1996]. A large decrease in growth was observed, particularly in high northern latitudes, in 1992. This feature has been attributed in part to decreased northern wetland emission rates resulting from anomalously low surface temperatures [*Hogan and Harriss*, 1994] and in part to stratospheric ozone depletion that increased tropospheric OH [*Bekki et al.*, 1994; *Fuglestvedt et al.*, 1994]. Records of changes in

the $^{13}C/^{12}C$ ratios in atmospheric CH_4 during this period suggest the existence of an anomaly in the sources or sinks involving more than one causal factor [Lowe et al., 1997; Mak et al., 2000].

There is no consensus on the causes of the long-term decline in the annual growth rate. Assuming a constant mean atmospheric lifetime of CH_4 of 8.9 years as derived by Prinn et al. [1995], Dlugokencky et al. [1998] suggest that during the period 1984 to 1997 global emissions were essentially constant and that the decline in annual growth rate was caused by an approach to steady state between global emissions and atmospheric loss rate. Their estimated average source strength was about 550 Tg y^{-1}.(Inclusion of a soil sink term of 30 Tg y^{-1} would decrease the lifetime to 8.6 years and suggest an average source strength of about 570 Tg y^{-1}.) Francey et al. [1999], using measurements of $^{13}CH_4$ from Antarctic firn air samples and archived air from Cape Grim, Tasmania, also concluded that the decreased CH_4 growth rate was consistent with constant OH and constant or very slowly increasing CH_4 sources after 1982. However, other analyses of the global methyl chloroform (CH_3 CCl_3) budget [Krol et al., 1998] and the changing chemistry of the atmosphere [Karlsdottir and Isaksen, 2000] argue for an increase in globally averaged OH of $+0.5\%$ y^{-1} over the last two decades and hence a parallel increase in global CH_4 emissions by $+0.5\%$ y^{-1}.

The historic record of atmospheric CH_4 obtained from ice cores has been extended to 420,000 years before present [Petit et al., 1999]. CH_4 varies with climate as does CO_2. High values are observed during interglacial periods, but these maxima barely exceed the immediate pre-industrial CH_4 mixing ratio of 700 ppb. At the same time, ice core measurements from Greenland and Antarctica indicate that during the Holocene CH_4 had a pole-to-pole difference of about 44 ± 7 ppb with higher values in the Arctic as today, but long before humans influenced atmospheric methane concentrations [Chappelaz et al., 1997]. Finally, study of CH_4 ice-core records at high time resolution reveals no evidence for rapid, massive CH_4 excursions that

might be associated with large-scale decomposition of methane hydrates in sediments [Brook et al., 2000].

1.3 Methane in the ocean

The oceans are believed to represent a source for atmospheric methane. This conclusion is based on the observation that the surface water of the ocean is usually supersaturated with respect to atmospheric methane. Supersaturation with methane has been observed at most stations in the world oceans. In order to understand the current global methane cycle, it is necessary to quantify its sources. At present, there remain large uncertainties in the estimated methane fluxes from sources to sinks. The ocean's source strength for atmospheric methane should be examined in more detail, even though it might be a relatively minor source, reported to be 0.005% to 3% of the total input to the atmosphere [Conrad and Seiler, 1988; Cicerone and Oremland, 1988; Bange et al., 1994].

Historically, the methane flux from the ocean has been estimated mainly from measurements of methane concentration in the surface water of the open oceans [Ehhalt, 1974]. In the open oceans, the surface water is slightly supersaturated with atmospheric methane. On the other hand, remarkable supersaturation in coastal regions, including continental shelf zones, has been reported. Owens et al. [1991] measured methane in the Arabian Sea and reported larger emission rate to the atmosphere (0.04 Tg y^{-1}), as compared with previous studies. Bange et al. [1994] re-evaluated the methane data in previous studies and reported that the degree of supersaturation was 200-500% in the Black Sea, 95-12,000% in the southern North Sea, and 120-23,900% in the northwestern Gulf of Mexico. Watanabe et al. [1994] showed that the flux of methane (3.8×10^2 mol CH_4 km^{-2} d^{-1}) in Funka Bay, Japan, was 2 to 3 orders of magnitude larger than values estimated in the open oceans [e.g., Cicerone and Oremland, 1988]. Tsurushima et al. [1996] reported that the flux of methane in the East China Sea was somewhat larger than oceanic values. Most of the known marine methane hydrate reservoirs are located along the continental margins

[*Gornitz and Fung*, 1994]. *Rehder et al.* [2000] reported that the enhancement of CH$_4$ fluxes to the atmosphere in regions of coastal upwelling is likely to occur on global scale. Although coastal seas occupy about 1/10 of the open ocean area [*Bange et al.*, 1994], the degree of supersaturation there is about 1 order of magnitude greater than that in the open oceans. However, methane data from coastal regions are too scarce to allow the global methane flux to be estimated precisely.

Several reports showed that the vertical profile of methane concentration has the maximum at subsurface layer in the Ocean but the origin of its maximum is not clear. Suggestion includes advection from nearby sources in shelf sediments, diffusion and/or advection from local anoxic environments, and in situ production by methanogenic bacteria, presumably in association with suspended particulate material. Some observations suggested that biogenic methane production occurred in the subsurface layer. In the water column, although only the methanogenic bacteria produce methane, they cannot survive under any traces of oxygen. Therefore, these bacteria are thought to probably live in the anaerobic microenvironments supplied by organic particles or guts of zooplankton [e.g., *Alldredge and Cohen*, 1987]. Recently, it is reported that some amount of methane is released by zooplankton-phytoplankton co-culture in the laboratory. But, there was few data that prove environmental subsurface methane production. In the Southern Ocean, large size zooplanktons such as Antarctic Krill and Sulpa live in great numbers, so in this area, much of methane seems to be formed in guts of zooplankton.

1.4 Objectives of this study

This study focused specially and temporally in detail profile of methane concentration and distribution in the water column. Fig. 1 shows the observation area taken up in this paper.

The Sea of Okhotsk taken up in chapter 2 has focused on the behavior of the oceanic biogenic methane in the coastal zone, the thermogenic methane off Sakhalin, and the effect of the Amur River water inflow. In addition in this chapter, it
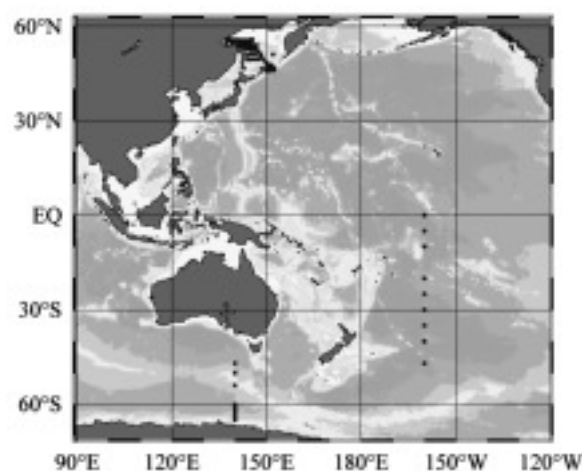

Fig. 1. Observation station taken up in this paper (XP98, XP99, XP2000, KH-01-3, JARE 43 Tangaroa cruise).

is indicated to be available taking the anomalously high methane concentration as a chemical tracer.

The South Pacific Ocean taken up in chapter 3 indicates that it focuses on the behavior of the methane in the open ocean, and that the concentration of methane in the open ocean increases gently in comparison with past and present surface water saturation.

The Southern Ocean taken up in the same chapter 3 has focused on the biogenic methane formed in the organic particle and guts of zooplankton. In this area, there is a good correlation of methane concentration with chlorophyll *a* concentration; it seems to be formed by Antarctic zooplankton.

While much of methane seemed to have been formed in these high latitude Oceans characterized by the high biological productivity in summer and the active vertical mixing in winter, the methane in the ocean hardly was observed. The estimates how much is the methane discharged to the atmosphere from these oceans are uncertainty. By clarifying spatial features of the marine methane supply to the atmosphere, it is a purpose of this study to reduce the uncertainty as a source of the ocean for atmospheric methane. Characteristics in each area are described at each following chapters.

Chapter 2   Methane in the western part of the Sea of Okhotsk in boreal summer 1998–2000

2.1   Introduction

The Sea of Okhotsk is one of the largest marginal seas, and is the important location for the ventilation of the North Pacific Intermediate Water characterized by a salinity minimum centered at 26.8 σ_θ. Therefore in recent years oceanographic studies have been made extensively [*Ohshima et al.*, 2002; *Mizuta et al.*, 2003]. *Lammers et al.* [1995] measured methane in the surface waters off the northeast coast of Sakhalin (52°30'–53°30'N, 143°20'–144°30'E) in the western part of the Sea of Okhotsk. They reported seasonal variations in the methane flux between the sea and the air due to methane concentrations ranging from 385 nM under the ice in winter to 6 nM in the ice-free midsummer. The magnitude of supersaturation indicates that the Sea of Okhotsk is a significant source of atmospheric methane. *Ginsburg et al.* [1993] reported gas hydrates and gas-vent fields in the Sea of Okhotsk on the northeastern continental slope off Sakhalin (53.2–54.6°N, 144.0–144.7°E), and *Cranston et al.* [1994] found methane hydrates of thermogenic origin there. Natural gas is extracted from the large oil and gas fields there (e.g., http://src-home.slav.hokudai.ac.jp/sakhalin/eng/71/akaha. html). Despite extensive seepage of thermogenic methane from sediments, there are only a few reports of the temporal and spatial variations in methane flux to the atmosphere and the processes controlling it.

As part of the Joint Japanese—Russian—U.S. Study of the Sea of Okhotsk, we measured methane concentrations throughout the water column in the western part of the Sea of Okhotsk during the three cruises in July–August 1998, August–September 1999, and June–July 2000 (Fig. 2). Here we report the distribution of methane released from sedimentary and thermogenic sources, and estimate the flux of methane from the western part of the Sea of Okhotsk to the atmosphere.
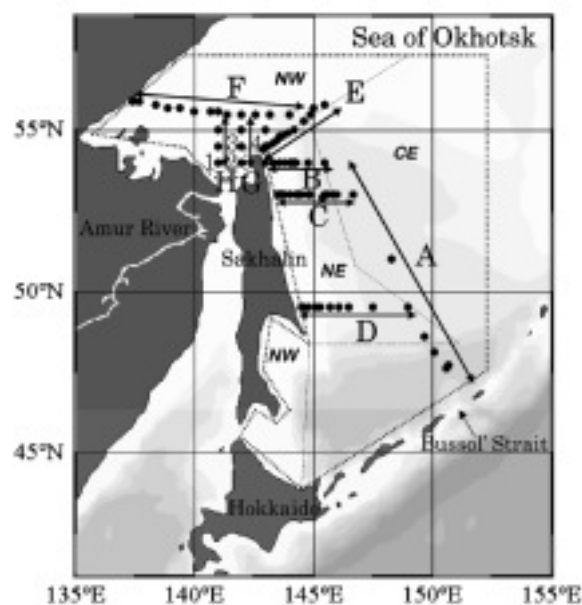

Fig. 2. Water sampling locations during the cruises of July–August 1998, August–September 1999, and June–July 2000. The dotted line shows the area where we estimated the methane flux between the sea and the air (see Table 2). The capital letters A to H indicate survey transects and the numbers 1 to 4 indicate the station for discussion (see Figure 15). NE means the area of northeastern Sakhalin shelf, NW means the area of the northwestern continental shelf, and CE means the central region of the Sea of Okhotsk.

2.2   Materials and Methods

During the three cruises, we collected about 1700 seawater samples at hydrographic stations (dots in Fig. 2), using the R/V Professor Khromov of the Far Eastern Regional Hydrometeorological Research Institute, Russia. In July–August 1998, the surface seawater samples were collected in a 1-L bucket, and other samples were collected from 5–25 depths from the surface (2 m) to the bottom in 10-L Niskin bottles. Each sample was carefully subsampled into a 30-mL glass vial so as to avoid contamination by air. The seawater samples were poisoned with 0.5 mL of mercuric chloride solution [*Tilbrook and Karl*, 1995; *Watanabe et al.*, 1995], and then the vials were closed with rubber and aluminum caps. They were stored in a cool, dark place until the gas chromatographic analysis of methane in our laboratory on land.

The analytical method was similar to that of

Tsurushima et al. [1996], briefly described here. The system consists of a purge and trap unit, a desiccant unit, rotary valves, a gas chromatograph (Shimadzu GC-8A) equipped with a flame ionization detector, and a data acquisition unit (Fig. 3). The whole volume of seawater in each 30-mL glass vial was processed all at once to avoid contamination and loss of methane [*Yoshida et al.*, 2004].

The precision obtained from replicate determinations of methane concentration was estimated to be better than 5% for the usual concentration of methane in seawater. The standard gases used contained 2.48 ppmv (Takachiho Chemical Industrial Co. Ltd) and 38.4 ppmv (Nippon Sanso Co. Ltd) of methane in pure nitrogen.

2.3 Results and Discussion

2.3.1 Methane distribution east of Sakhalin

East of Sakhalin, the methane concentrations showed prominent features in waters close to the bottom and between the subsurface and surface mixed layers.

2.3.1.1 Thermogenic methane in waters over the northeastern shelf

In waters over the northeastern shelf, anomalously high concentrations of methane were observed near the bottom (Figs. 4-6) of the eastern shelfbreak at a depth of ~200 m, due to methane seepage from an underlying oil field [*Ginsburg et al.*, 1993; *Lammers et al.*, 1995]. Maximum emission rate of methane from sediments was estimated based on maximum concentration of methane and flow rate of seawater (Table 1). The highest concentration of methane existed in water with a density of 26.6–26.8 σ_θ (corresponding to the Okhotsk Sea Intermediate Water), a relatively low temperature, a low nitrate concentration, and a high dissolved oxygen concentration every year (Fig. 7). The anomalously high concentrations of methane oc-
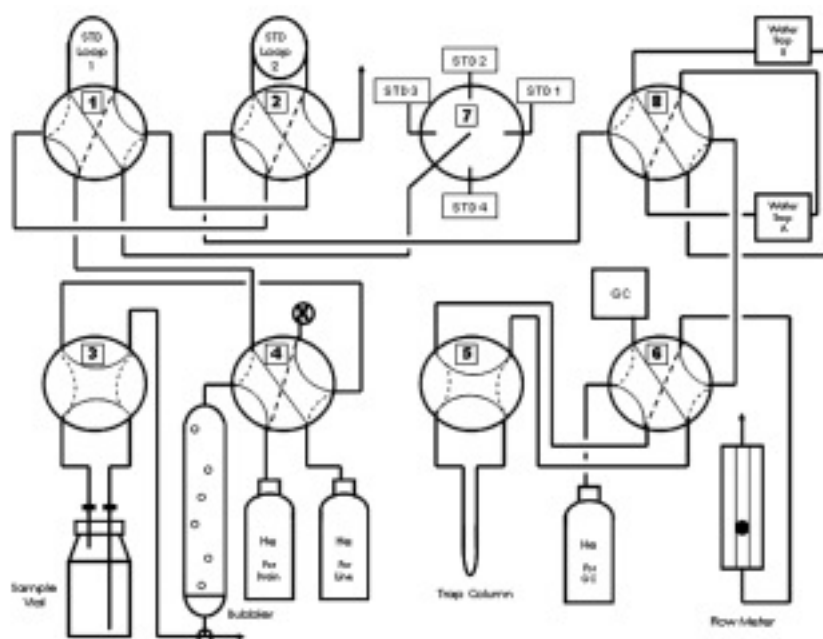

Fig. 3. Flow diagram of the gas chromatograph analysis.

Table 1. Maximum CH_4 emission rate from sediments (mg CH_4 m^{-2} d^{-1})

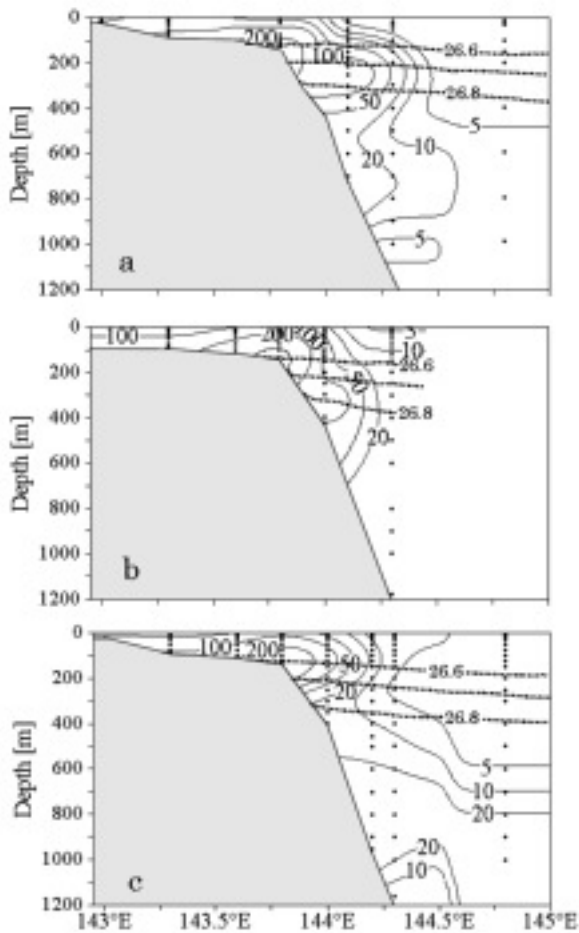| Section	year		
	1998	1999	2000
B	1.8	4.1	2.3
C	2.0	0.8	1.7
D	0.3	0.2	0.3

Fig. 4. Distribution of methane concentrations along
        section B in (a) July–August 1998, (b) August–
        September 1999, and (c) June–July 2000. The
        dotted lines show water with a density of 26.6–
        26.8 σ_θ.
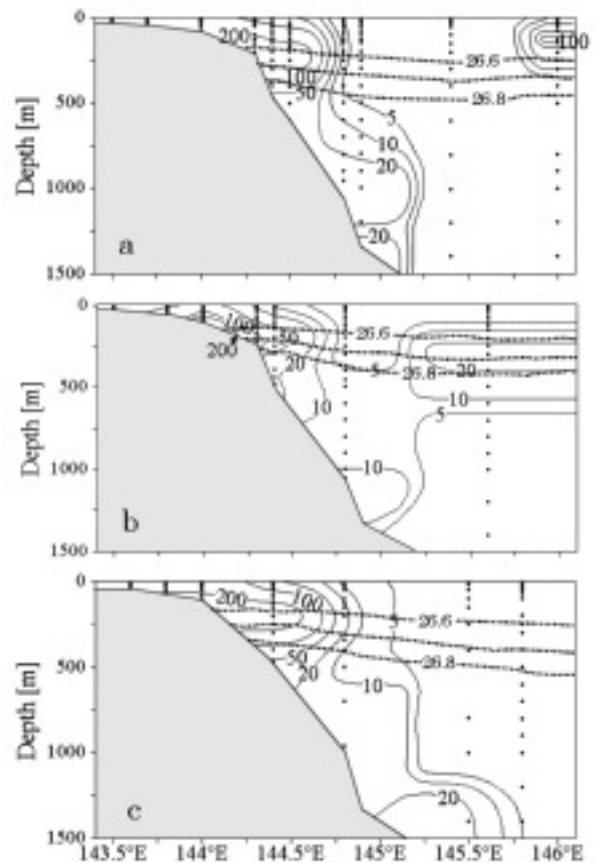

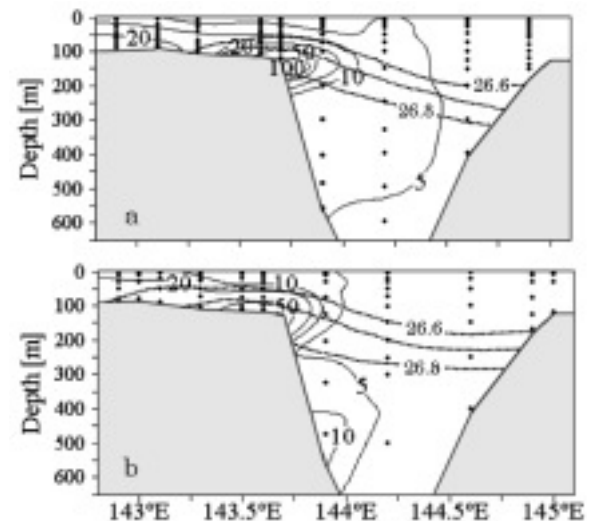Fig. 5. As for Figure 4 except in section C.

Fig. 6. Distribution of methane concentrations along
        section E in (a) August–September 1999, and (b)
        June–July 2000. The dotted lines show water
        with a density of 26.6–26.8 σ_θ.

curred among the dense shelf water, which is
probably originated from the northwestern shelf
area and transported by the East Sakhalin Cur-
rent [e.g., *Kitani*, 1973; *Talley*, 1991; *Yamamoto et
al.*, 2002].

The methane concentration in the near-bottom
water along section E was relatively low compar-
ed with those of sections B and C to the south,
showing clearly that the thermogenic methane
sources are not uniformly distributed geographi-
cally along the shelf northeast of Sakhalin. The
highest methane concentration in sections B and
C varied temporally and spatially: 488 nmol kg^{-1}
in July–August 1998 (section C), 981 nmol kg^{-1} in
August–September 1999 (section B), and 556 nmol
kg^{-1} in June–July 2000 (section B). There are
two possible sources of changes in methane con-

centration: variations in methane flux from thermogenic sources and lateral transport by the East Sakhalin Current.

The highest methane along section C, east of 145.5°E, was found in subsurface water with a density of 26.6–26.8 σ_θ in 1998 and 1999, but not in 2000 (Fig. 5). In open oceans, the highest methane concentration is commonly found in the subsurface water [e.g., *Ward et al.*, 1987; *Conrad and Seiler*, 1988], as explained by a decrease in biological methane production with depth [*Karl and Tilbrook*, 1994] and a high rate of loss from the surface layer [*Jayakumar et al.*, 2001]. Along section C, the subsurface maximum concentration of methane was too high to explain by in situ production via biological activities. In the northeastern Sea of Okhotsk, extremely high concen-

trations of methane caused by major thermogenic methane sources have also been reported [*Lammers et al.*, 1995, based on *Geodekyan et al.*, 1976]. The subsurface maximum east of 145.5°E may have been caused by the southwestward transport of thermogenic methane from northeastern latitudes [*Ohshima et al.*, 2002].

Along section D (Fig. 8), at stations close to Sakhalin (west of 146°E), the maximum methane concentration (61 nmol kg^{-1}) occurred in water with a density of 27 σ_θ in July–August 1998. This result also indicates relatively large thermogenic methane emission for the year. As found in the area northeast of Sakhalin, these methane concentrations varied significantly from year to year: 43 nmol kg^{-1} in August–September 1999, 80 nmol
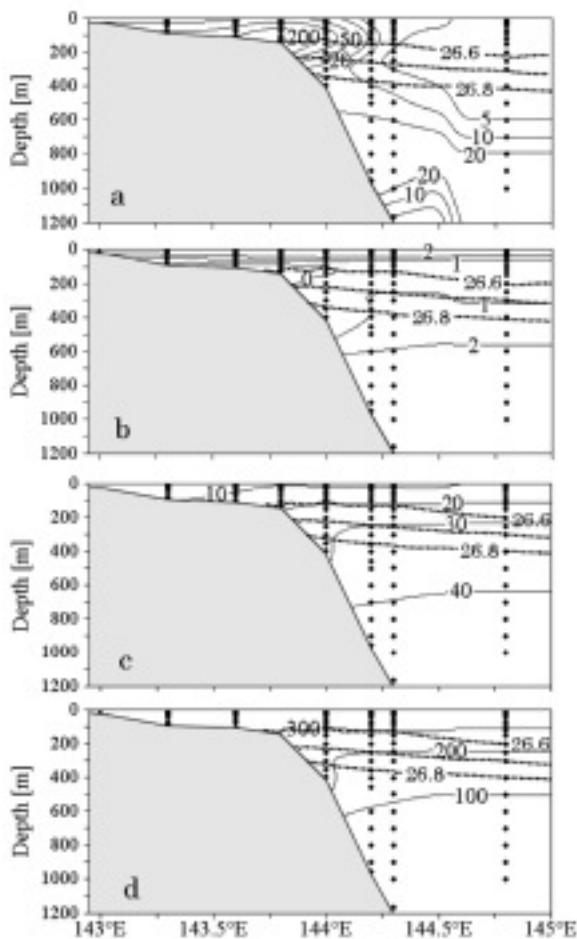

Fig. 7. (a) Distribution of methane, (b) temperature, (c) nitrate concentration, and (d) dissolved oxygen concentration along section B in June–July 2000. The dotted lines show water with a density of 26.6–26.8 σ_θ.
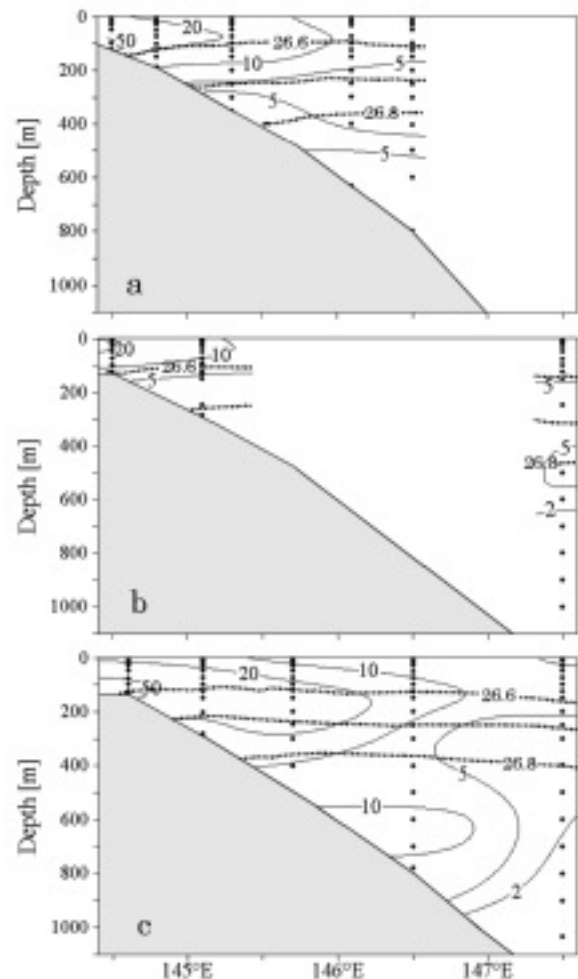

Fig. 8. Distribution of methane concentrations along section D in July–August 1998, August–September 1999, and June–July 2000. The dotted lines show water with a density of 26.6–26.8 σ_θ.

kg⁻¹ in June–July 2000.

2.3.1.2 Methane distribution in surface sea-water

Surface seawater over the shelf northeast of Sakhalin, the methane concentration had ranged from 3 to 42 nmol kg⁻¹ in July–August 1998, from 3 to 14 nmol kg⁻¹ in August–September 1999, and from 4 to 80 nmol kg⁻¹ in June–July 2000 (Fig. 9). In a layer of 50–200 m depth of the western part, its concentration showed a steep gradient between the subsurface and surface mixed layers, while in the eastern part remained fairly constant. In the eastern part of sections B and C and the northern part of section A, the methane concentrations in the surface mixed layer (~20 m) ranged from 3 to 5 nmol kg⁻¹, approximately equal to or slightly larger values reported in the open oceans (Figs. 7, 8, and 10).
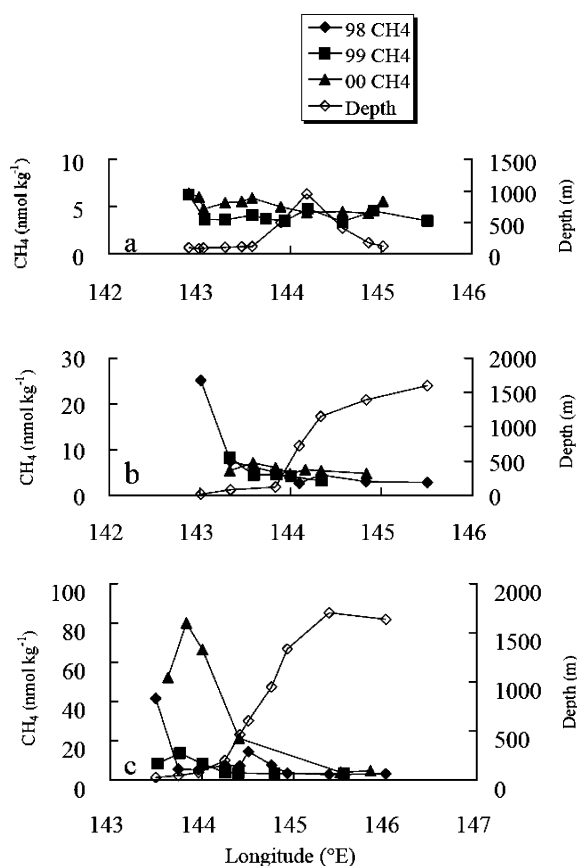
Along the eastern Sakhalin coast, the existence

of less-saline surface seawater originating from the Amur River has been reported [*Itoh and Ohshima*, 2000]. From the vertical profiles of temperature and salinity, a strong stratification in the upper ~10 m (an example is shown in Fig. 11) was observed. We surmise that the strong stratification due to freshwater inputs from the Amur River restricted the underlying methane-rich water from ventilating. For example, along section C, freshwater input from the Amur River was observed in August–September 1999, but not clearly in June–July 2000.

Consequently, the surface methane concentration was relatively low in 1999, while high in 2000, although the 1999 maximum methane concentration in the near-bottom water was larger than that in 2000 (Fig. 12).

Relatively high concentrations of methane were observed at almost all the stations with the shallowest depth (< ~100 m) near the coast. From the observations of near-surface circulation and tidal currents in the Sea of Okhotsk, *Ohshima et al.* [2002] have found amplification of the diurnal tidal current near the coastal region east of Sakhalin. Their observational results suggest that the high methane concentration in the sur-
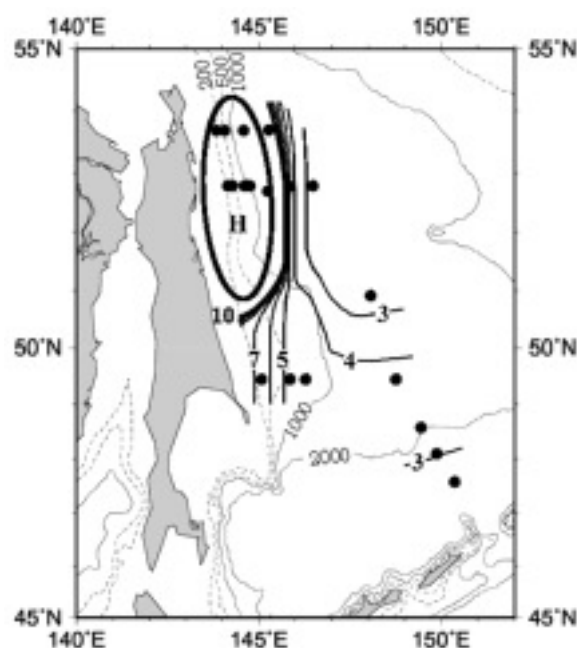

Fig. 9. Longitudinal distributions of methane in surface seawater and bottom depth along (a) section E, (b) section B, and (c) section C over the shelf northeast of Sakhalin.

Fig. 10. Distribution of methane concentrations in water with a density of 26.8 σ_θ in July–August 1998.
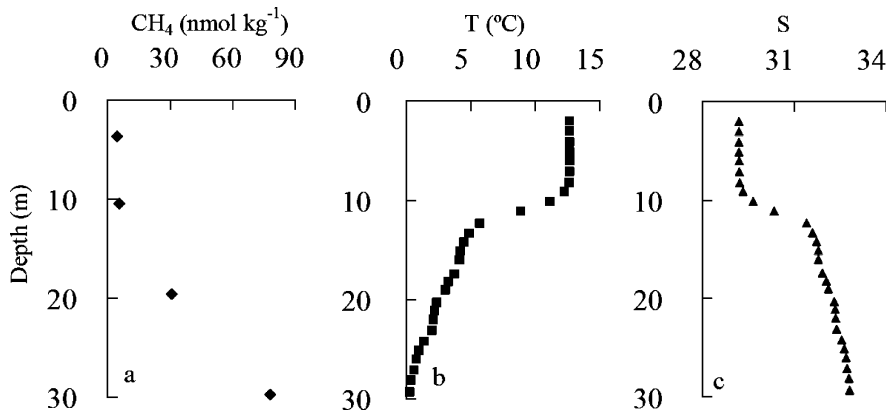
CH$_4$ (nmol kg^{-1})

T (°C)

S

Fig. 11. Vertical profiles of (a) methane concentration, (b) emperature, and (c) salinity in the upper 30 m over the shelf northeast of Sakhalin (54°N, 143.8°E).
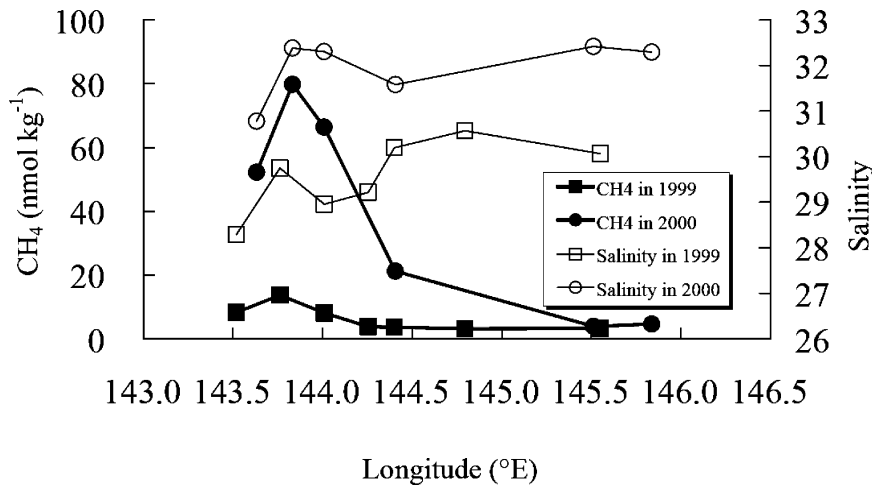
Longitude (°E)

Fig. 12. Distributions of methane and salinity in surface water along section C in August–September 1999 and June–July 2000.

face water observed near the coastal region may be caused by the active tidal mixing there. As another possibility for the high methane concentration of the coastal surface water, a wind-driven mixing effect should be relatively small, because of weak wind in summer.

2.3.1.3 Vertical profile of methane concentrations in the central region

The anomalously high methane concentrations along sections B and C can be used to trace the water with a density of 26.6–26.8 σ_θ in the East Sakhalin Current. Methane distribution in such water in 1998 showed higher concentrations (>7 nmol kg^{-1}) over the shelf east of Sakhalin (Fig. 10). In the central region north of 50°N, the methane concentration east of the shelfbreak

decreased considerably to the level of 3 nmol kg^{-1}, while south of 50°N relatively high concentration ($\sim$5 nmol kg^{-1}) was observed. This distribution of methane was mainly controlled by the transport of methane from the source region in the shelf northeast of Sakhalin. The East Sakhalin Current can be divided into two parts, southward flow along the coast and southeastward flow away from the coast of Sakhalin [*Ohshima et al.*, 2002]; our results also support its current pattern.

2.3.2 Methane distributions in the northwestern continental shelf zone

2.3.2.1 Methane north of Sakhalin

North to northwest of Sakhalin (section F), the methane concentration in the near-bottom water

was higher than that in the surface water and fairly constant over a wide area north of 54.5°N (Fig. 13). The methane is thought to be discharged by microorganisms in the sediments into the water column [*Ward et al.*, 1987; *Conrad and Seiler*, 1988; *Kvenvolden et al.*, 1993; *Bange et al.*, 1994, 1998; *Tsurushima et al.*, 1996; *Jayakumar et al.*, 2001]. This is a common feature of methane production in waters over continental shelves, and
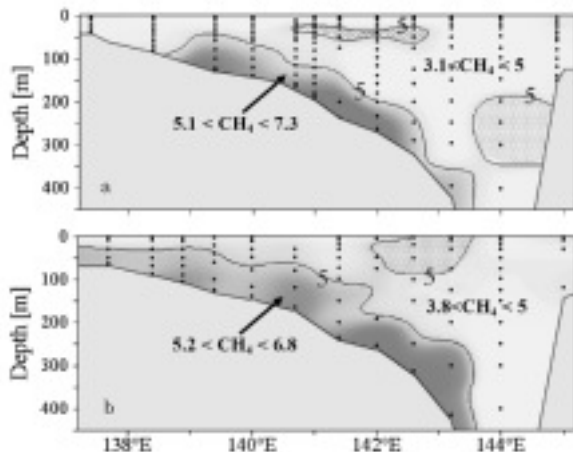

Fig. 13. Distribution of methane concentrations along section F in August–September 1999 (upper panel) and June–July 2000 (lower panel). The dotted lines show water with a density of 26. 6–26.8 σ_θ.

is the reason why this area acts as an important oceanic source.

2.3.2.2 Methane distribution near the Amur's mouth

As found in surface salinity at Stations 1 and 2 (Figs. 2 and 14), freshwater from the Amur River mostly flows toward the east. A lot of organic matter from the Amur River is carried east to the west coast of Sakhalin, as supported by the measurements of turbidity. Because of the shallow depths, organic substances are considered to be accumulated in the sediments without decomposition. The maximum concentration in the near-bottom water was 32 nmol kg^{-1} at 142°E (Station 2) and 7 nmol kg^{-1} at 141°E (Station 1) in August–September 1999 (not shown), and 98 nmol kg^{-1} at 142°E and 10 nmol kg^{-1} at 141°E in June–July 2000 (Fig. 14). *Rehder et al.* [2002] discussed the large methane concentration in connection with particle concentration off Oregon. Our results suggest that the high concentration of methane over this continental shelf is at least caused by the biogenic methane.

The methane concentration in the surface water was not correlated with salinity (Fig. 15).
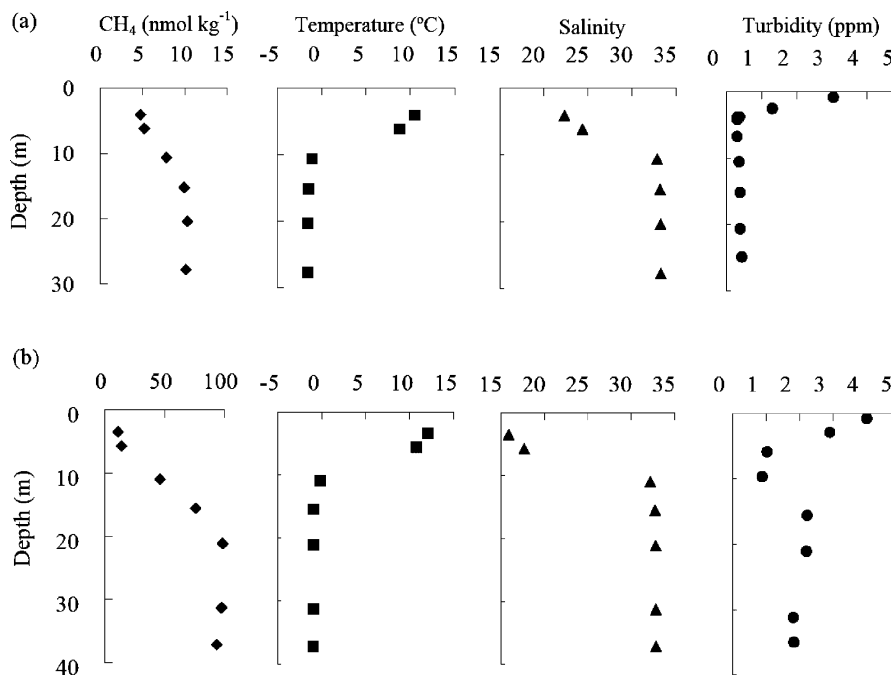

Fig. 14. Vertical profiles of methane concentration, temperature, salinity, and turbidity at 54°N, 141°E in August–September 1999 (a) and 54°N, 142°E in June–July 2000 (b).
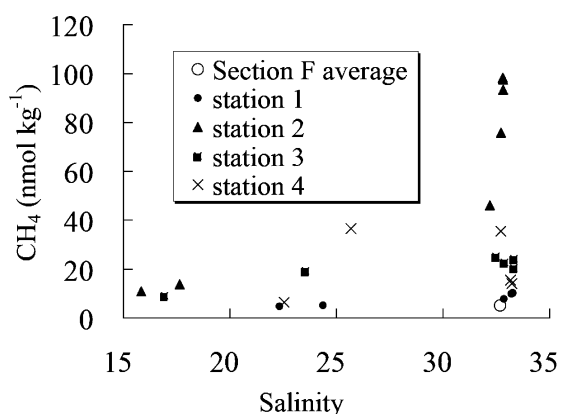
Fig. 15. Methane concentration against salinity in water over the northwestern continental shelf (section F average and station 1 to 4) in June–July 2000.

This result is completely different from that observed in the Mandovi estuary, Gõa, India [*Jayakumar et al.*, 2001], where large riverine inputs of methane mean that the methane concentration increases as the salinity decreases.

2.3.3 Methane flux between sea and air in the western Sea of Okhotsk

The degree of saturation (in %; 100% = equilibrium) was calculated from the observed concentration of methane, Cw, and the concentration of methane in water equilibrated with ambient air at in situ conditions, Ca, which can be obtained from the mole fraction in dry air by using a solubility equation of *Wiesenburg and Guinasso* [1979]. We used 1.80 ppmv as the atmospheric methane concentration [*Tans et al.*, 2002].

Degree of methane saturation
$$= 100 \times (Cw/Ca). \qquad (1)$$
The air-sea exchange flux of methane (F) can be expressed as:
$$F = kw \times (Cw - Ca), \qquad (2)$$
where kw is the gas transfer coefficient. To get kw, we assumed a quadratic kw-wind speed (v) relationship established by *Wanninkhof* [1992]:

$$k_w = 0.39 v^2 \cdot \left(\frac{Sc}{660}\right)^{-\frac{1}{2}}, \qquad (3)$$

where Sc is the Schmidt number of methane, which is defined as the ratio of the kinematic viscosity of water to the diffusion coefficient of methane. By using equations (2) and (3), we calculated the methane fluxes at in situ water

temperature, salinity, and mean wind speeds acquired from the Japan Meteorological Agency [*GANAL*, 1998, 1999, 2000]. The wind speeds used in this work were averages during the periods of observations.

The relative error associated with kw determined by equation (3) is about 25%, assuming a 10% error on the Schmidt number [*Wanninkhof*, 1992] and using the measured variability in the wind speeds while sampling.

We calculated the methane flux between the sea and the overlying air in the western Sea of Okhotsk (Table 2). Owing to the effect of temperature on methane solubility [*Wiesenburg and Guinasso*, 1979], the degree of saturation was not as large as calculated at lower latitudes. The average value of the methane flux was 6.5 mol km^{-2} d^{-1} (range, 0.4 to 88 mol km^{-2} d^{-1}), which is comparable to values of coastal and shelf regions [*Bange et al.*, 1994; *Tsurushima et al.*, 1996] and larger than those of the open ocean [*Kiene*, 1992; *Bange et al.*, 1994]. The western part of the Sea of Okhotsk can be divided into 3 areas (Fig. 2); in the central region of the Sea of Okhotsk, with depths deeper than 1000 m (section A), northwestern continental shelf region (sections F, G, and H), and east Sakhalin Shelf region (sections B, C, D, and E). Along section A, the methane flux (1.6 mol CH$_4$ km^{-2} d^{-1}) was somewhat larger than those (0.3 to 6.9 mol CH$_4$ km^{-2} d^{-1}) of the open ocean [*Kiene*, 1992; *Bange et al.*, 1994]. The northwestern continental shelf region, where methane is released from sedimentary sources, showed higher methane flux values (2.1 to 2.9 mol CH$_4$ km^{-2} d^{-1}) than those of section A. In the northeastern Sakhalin Shelf region, the methane flux (5.8 to 12.2 mol CH$_4$ km^{-2} d^{-1}) was remarkably high.

The emission rate of methane was calculated to be 0.004 to 0.008 Tg CH$_4$ y^{-1} in the shelf northeast of Sakhalin affected by thermogenic sources, 0.003 to 0.005 Tg CH$_4$ y^{-1} in the area of the northwestern continental shelf affected by sedimentary sources, and 0.004 Tg CH$_4$ y^{-1} in the central region (Tables 2–3). On the assumption of an average wind velocity of 7 m s^{-1} throughout the year, *Lammers et al.* [1995] estimated a

Table 2. Surface methane concentrations, methane saturation, wind speed, and air-sea flux at each location in the western Sea of Okhotsk.

Region	Cruise year	Section	Methane concentration (nmol kg^{-1})		Methane saturation (%)		Wind speed (m s^{-1})		Air-sea flux (mol CH$_4$ km^{-2} d^{-1})		$''$
			mean	range	mean	range	mean	range	mean	range	
Central	1998	A	3.6± 0.6	3.0- 4.6	139	116- 175	4.8	4.1-5.2	1.6	0.68-3.4	7
Shelf Northeast of Sakhalin	1998	B	7.3± 8.0	2.7-25.1	278	112- 905	3.7	2.7-4.1	3.5	0.36-11	7
	1999	B	5.0± 1.9	3.2- 8.2	191	127- 313	6.2	6.2-6.2	7	2 -16	5
	2000	B	5.6± 0.8	4.8- 7.1	196	165- 251	5.1	5.0-5.4	4.9	3.4 - 7.7	7
	1998	C	9.9±11.6	2.8-41.5	390	120-1523	3.7	3.4-4.1	7.3	0.57-33	10
	1999	C	5.1± 4.0	3.2- 8.3	197	128- 316	6.1	5.6-6.7	9.3	2.5 -25	7
	2000	C	38.1±32.6	4.0-79.8	1192	129-2440	4.8	4.5-5.2	43	1.4 -88	6
	1998	D	9.3± 5.5	3.5-14.9	349	144- 564	3.7	3.1-4.5	6.3	1.8 -13	4
	1999	D	7.6± 5.4	3.1-13.6	293	124- 507	6.7	6.1-7.3	12	2.5 -30	3
	2000	D	6.9± 2.2	4.1-10.4	212	127- 313	4.9	4.7-5.1	4.9	1.3 - 8.8	5
	1999	E	4.1± 0.9	3.4- 6.3	144	116- 229	6.2	5.7-6.6	3.2	1.3 - 8.1	10
	2000	E	5.3± 0.7	4.3- 6.5	169	127- 217	5.0	4.7-5.1	3.3	1.4 - 5.4	11
							weighted average:		8.6		
Northwestern continental shelf	1999	F	3.7± 0.4	3.1- 4.4	138	117- 152	5.4	3.7-6.3	2.1	0.78- 3.3	10
	2000	F	4.4± 0.6	3.8- 5.7	146	129- 182	4.2	2.6-5.1	1.5	0.47- 4.1	10
	1999	G	4.4± 0.4	4.1- 4.7	155	147- 163	5.0	4.4-5.7	2.8	2.6 - 2.9	2
	2000	G	8.2± 4.7	4.5-10.9	283	156- 377	4.4	3.7-4.7	7.9	2.5 -11.0	3
	1999	H	3.7± 0.4	3.4- 4.1	136	126- 147	5.2	4.4-5.5	1.8	1.6 - 2.0	3
	2000	H	4.9± 1.1	3.8- 6.1	168	128- 211	4.4	3.9-4.6	2.6	1.1 - 4.7	3
							weighted average:		2.5		

Table 3. Emission rate of methane in the western Sea of Okhotsk in boreal summer

	Area code	Area (km^2)	Emission rate of methane (TgCH$_4$y^{-1})			
			1998	1999	2000	mean
Shelf northeast of Sakhalin	NE	0.11×10^6	0.004	0.005	0.008	0.006
Northwestern continental shelf*	NW	0.25×10^6	—	0.003	0.005	0.004
Central	CE	0.42×10^6	0.004	—	—	0.004
Total		0.78×10^6	—	—	—	0.014

*South of Sakhalin the flux was considered to be equal to that in the shelf northeast of Sakhalin (see Figures 2-7).

methane flux of 0.13 Tg CH$_4$ y^{-1} in the Sea of Okhotsk on the basis of measurements on the shelf northeast of Sakhalin in winter and summer. By calculating averages for each region, the emission rate in the western Sea of Okhotsk (0.78 × 10^6 km^2, ~55% of total) was estimated to be 0.014 Tg CH$_4$ y^{-1} in boreal summer. In comparison with the results of *Lammers et al.* [1995], we observed both relatively low supersaturation of methane in surface water stood on wide-ranging observations and smaller wind speeds based on objective analysis (Table 2).

Methane and freshwater originating from the Amur River control the sea-air methane flux in the western Sea of Okhotsk, which is supposed to vary greatly on a time scale from months to years. Therefore, repeated measurements are necessary in order to estimate more precisely the annual methane flux in the Sea of Okhotsk. Along the east coast of Sakhalin, the methane flux at stations close to land (< ~100 m, Fig. 16) was generally larger than those in the deeper shelf east of Sakhalin. As mentioned above, thermogenic methane was effectively transported to the surface by tidal mixing.

Therefore, tidal mixing plays an important role in increasing the methane flux over the shelf east of Sakhalin. On the basis of high methane concentrations observed below the ice cover in *March* 1991, *Lammers et al.* [1995] suggested that the seasonal ice cover in the Sea of Okhotsk induces a peak flux of accumulated methane as it
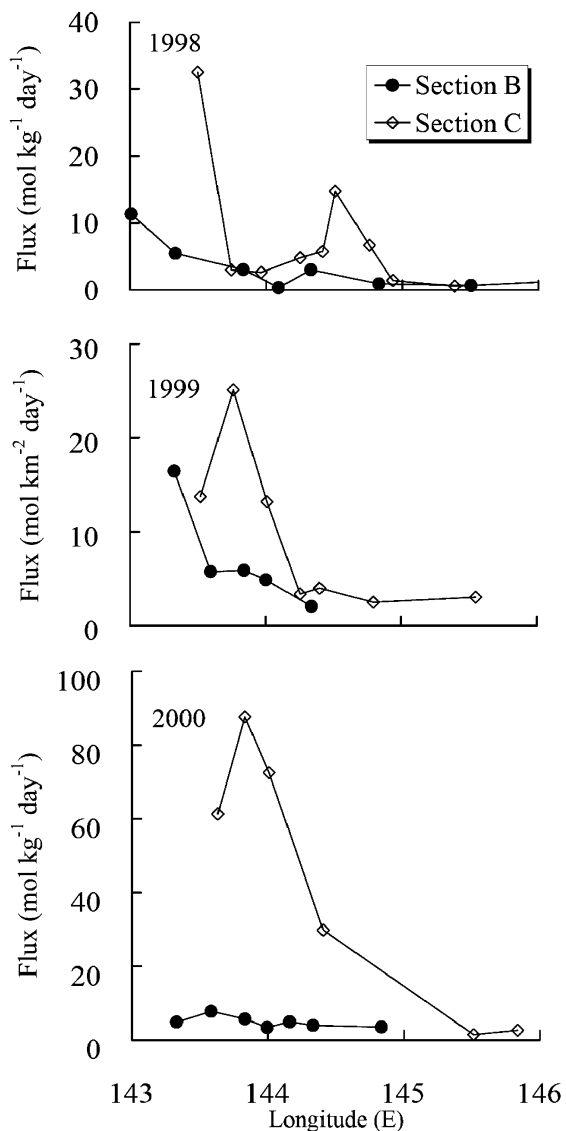
Fig. 16. Longitudinal distributions of methane flux between the sea and the air over the shelf northeast of Sakhalin.

retreats. However, our results suggest that because stratification remains in areas deeper than 50 m, the methane-rich water hardly ventilates, which fact could cause less methane flux than expected from the high methane concentrations below the surface. It is, of course, necessary to examine the seasonal variation in surface methane concentration in order to discuss the sea-air methane flux further in detail.

2.3.4 Vertical and lateral transport of methane off east Sakhalin

During the southward flow of the East Sakhalin Current, the methane concentration in the surface water generally increased from section B to section C (Fig. 9). The methane flux between the sea and the air was not large enough to establish equilibrium during the southward flow, which had an average speed of 0.3–0.4 m s^{-1} [*Ohshima et al.*, 2002]. By assuming a flow speed of 0.3 m s^{-1} and using the average methane flux of the 2 sections (Table 1), we calculated the amount of methane added to the surface between sections B and C to be 4 nmol kg^{-1} in August–September 1998, 2 nmol kg^{-1} in July–August 1999, and 40 nmol kg^{-1} in June–July 2000. If the methane was transported by vertical diffusion, then the methane flux, Q, from the subsurface to the surface mixed layer is calculated as:

$$Q = -Dz \cdot \left(\frac{\Delta C}{\Delta Z}\right), \qquad (4)$$

where Dz is the vertical diffusion coefficient and ($\Delta C/\Delta Z$) is the vertical gradient of the methane concentration. The diffusion coefficient was calculated to be 0.1–0.4 cm^2 s^{-1} in August–September 1998 and July–August 1999, and about 1 order of magnitude larger ($\sim$1 cm^2 s^{-1}) in June–July 2000. This analysis may be too simple for a discussion of the vertical transport of methane off east Sakhalin, but it clearly shows the decreasing effect of stratification due to freshwater inputs from the Amur River on the methane transport from the subsurface to the surface mixed layer.

To determine the oxidation rate of methane, we obtained the amount of methane in a water column by integrated methane concentration from the surface to the bottom along section C and D. Then we calculated the whole amount of methane in a 1-m strip of water from 143.5° to 144.8°E along section C, and from 144.5° to 149.0°E along section D (Table 4), because the East Sakhalin Current flows south mainly and to southeast above a gently sloping bottom [*Ohshima et al.*, 2002; *Mizuta et al.*, 2003] and no linear relationship between methane concentration and temperature indicating diffusion are plotted in Fig. 17.

From the amount of methane emitted to the atmosphere over 16 days, and by assuming a flow speed of 0.3 m s^{-1} between the 2 sections and a first-order reaction, we estimated the half-life of

Table 4. Amount of methane (g) in whole water column
in a 1-m strip along sections C and D.

Section	Latitude	1998	1999	2000
C	143.5°–144.8°E	41,308	9,509	43,687
D	144.5°–149.0°E	14,999	—	25,928

*From sections C to D, the amount of methane emitted to the atmosphere was estimated to be 441 g CH$_4$ in July–August 1998 and 1972 g CH$_4$ in June–July 2000.
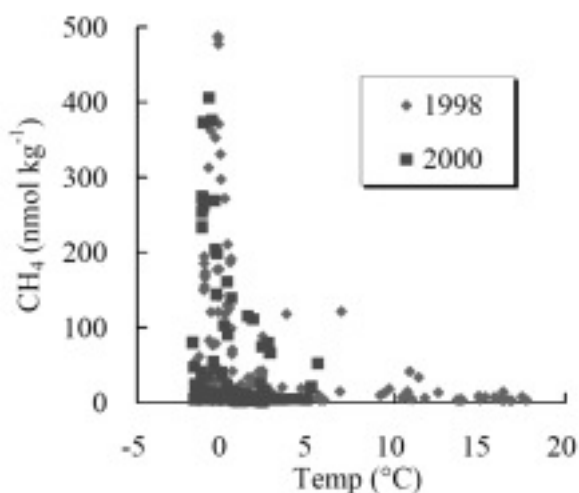
Fig. 17. Methane concentration vs. water temperature along section C to D in 1998 and 2000.

methane oxidation as 15 days in July–August 1998 and 30 days in June–July 2000. We did not estimate the half-life in July–August 1999, since only a few data were obtained along section C. High rates of microbial methane oxidation in seawater were reported in areas that contain high methane [*Nakamura et al.*, 1994; *Valentine et al.*, 2001]. Our results are compatible with those previous results. In order to use methane as a quantitative chemical tracer, it will be necessary to experimentally determine the biological oxidation rates of methane just after the collection of sample seawater.

2.4 Summary

In the Joint Japanese—Russian—U.S. Study of the Sea of Okhotsk, oceanic methane concentrations were measured in order to examine the distribution of methane, variations in its concentration, and the sea-air methane flux in the western part of the Sea of Okhotsk in July–August 1998, August–September 1999, and June–July 2000. Contrary to the earlier report in the Man-

dovi estuary, Gõa, India [*Jayakumar et al.*, 2001], fresh eater inputs from the Amur River showed relatively low concentration of methane. In waters over the shelf northeast of Sakhalin, anomalously high concentrations occurred in the near-bottom water (26.6–26.8 σ_θ) at the eastern edge of the broad shelf (~200 m), owing to methane seepage from an underlying oil field [*Ginsburg et al.*, 1993; *Lammers et al.*, 1995]. This allowed us to trace the East Sakhalin Current flowing southward along the coast and southeastward away from Sakhalin on a time scale of a few months. In the area with depths of 50–200 m, freshwater inputs from the Amur River led to strong stratification, which restricted the methane-rich subsurface water from ventilating. The coefficient of vertical diffusion from the subsurface to the surface mixed layer in the same area was calculated to be 0.1–0.4 cm^2 s^{-1} with a freshwater cap, and about 1 order of magnitude smaller without a freshwater cap. Along the east Sakhalin coast where the depth is shallower (<~100 m), tidal currents enhanced the vertical transport of methane-rich water to the surface.

In the area of the northwestern continental shelf, methane was discharged from sediments to the water column, especially off the east coast of Sakhalin, where a lot of organic matter from the Amur River is accumulated without decomposition. In the central region of the Sea of Okhotsk, the methane concentration showed a broad maximum in water with a density of 26.6–26.8 σ_θ, owing to in situ production of methane, as found in the open oceans and in the southeastward arm of the East Sakhalin Current.

In the area of the shelf northeast of Sakhalin (0.11 × 10^6 km^2), which is affected by thermogenic sources, the emission rate of methane was calculated to be 0.006 Tg CH$_4$ y^{-1}. In the northwest-

ern continental shelf region (0.25 $\times$ 10^6 km^2), which is affected by sedimentary sources, it was calculated to be 0.004 Tg CH$_4$ y^{-1}. In the central region of the Sea of Okhotsk (0.42 $\times$ 10^6 km^2), where the area has a larger flux of methane than in the open oceans, it was estimated to be 0.004 Tg CH$_4$ y^{-1}. Thus, in the western Sea of Okhotsk (0.78 $\times$ 10^6 km^2, 55% of total), the emission rate of methane was calculated to be 0.014 Tg CH$_4$ y^{-1} in boreal summer.

By taking into account the methane budget along section C from 143.5° to 146.0°E and along section D from 144.5° to 149.0°E, we estimated the half-life of methane oxidation to be about a month (15–30 days) by assuming the first order reaction of methane.

Chapter 3 Methane in the South Pacific and Southern Ocean in austral summer 2001–2002

3.1 Introduction

To estimate an accurate amount of the methane exchange from ocean to atmosphere, it is necessary to examine process controlling surface methane concentration widely and vertically. Several reports showed that vertical profile of methane concentration has the maximum at subsurface layer in the Ocean [e.g., *Scranton and Brewer*, 1977; *Watanabe et al.*, 1995; *Kelley and Jeffrey*, 2002]. There have been made some suggestion about the origin of the subsurface maximum, advection from nearby sources in shelf sediments, diffusion and/or advection from local anoxic environments, and in situ production by methanogenic bacteria, presumably in association with suspended particulate material. In the open ocean, some observations indicated that biogenic methane production occurred in the subsurface layer. The methanogenic bacteria produce methane in the seawater, but they cannot survive under any traces of oxygen. Therefore, these bacteria are thought to probably live in the anaerobic microenvironments supplied by organic particles or guts of zooplankton [e.g., *Alldredge and Cohen*, 1987]. The methanogens also appear to be zooplankton species-specific [*de Angelis and Lee*, 1994], which further contributes to the lack

of a consistent correlation between seawater methane concentration and measured biological parameters [*Burke et al.*, 1983]. Recently, it is reported that some amount of methane is released by zooplankton-phytoplankton co-culture in the laboratory. But, there are only a few data that prove environmental subsurface methane production. Methane production in surface seawater is balanced by microbial oxidation [*Ward et al.*, 1987; *Jones*, 1991] and sea-air exchange. Open ocean turnover times with respect to biological oxidation are of the order of year [*Ward et al.*, 1987; *Jones*, 1991; *Kiene*, 1991], which suggests that sea-air exchange is the major sink for seawater methane. So, this study investigates in detail profile of methane concentration and distribution in the water column in the South Pacific as an open ocean and the Southern Ocean as one of the most biologically productive regions characterized by large scale zooplankton such as Antarctic Krill and Sulpa (Fig. 18). Moreover, observations are performed to address the temporal variation of oceanic methane at the same transect in the Southern Ocean, aboard the R/V Hakuho Maru and the R/V Tangaroa.

3.2 Materials and Methods

We collected about 1000 seawater samples at hydrographic stations in the South Pacific along 160°W and in the Southern Ocean along 140°E (dots in Fig. 1), using the R/V Hakuho Maru of
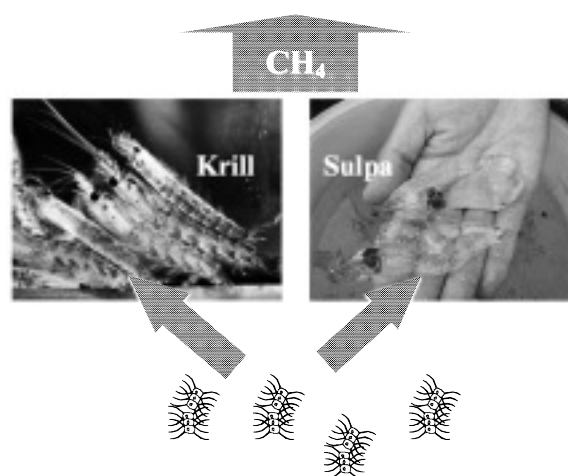

Fig. 18. The conceptual scheme of the methane production from the phytoplankton-zooplankton.

the Ocean Research Institute, University of Tokyo as KH-01-3 cruise (December 2001 in the South Pacific and January 2002 in the Southern Ocean) and using R/V Tangaroa of National Institute of Water and Atmospheric Research, New Zealand as the 43rd Japanese Antarctic Research Expedition Marine Science Cruise (February 2002 in the Southern Ocean along the same transect of Hakuho Maru Cruise).

The surface seawater samples were collected in a 1-L bucket, and other samples were collected from 5-25 depths from the surface (~10 m) to the bottom in 12-L Niskin bottles. Each sample was carefully subsampled into a 30-mL glass vial so as to avoid contamination by air. The seawater samples were poisoned with 20 μL of mercuric chloride solution [*Tilbrook and Karl*, 1995; *Watanabe et al.*, 1995], and then the vials were closed with rubber and aluminum caps. They were stored in a cool, dark place until the gas chromatographic analysis of methane on board or in our laboratory on land.

The analytical method was equal to that in the study for the Sea of Okhotsk (see Chapter 2). The standard gases used contained 2.02, 19.6, and 38.4 ppmv (Nippon Sanso Co. Ltd) of methane in pure nitrogen.

3.3 Results and Discussion

3.3.1 Methane in the South Pacific

3.3.1.1 Methane distribution and saturation

At each station, the surface methane was supersaturated with respect to the methane in the air (Fig. 19). The equatorial region had higher saturation ratio than more southerly sites. The surface methane concentration increased by 1 nmol
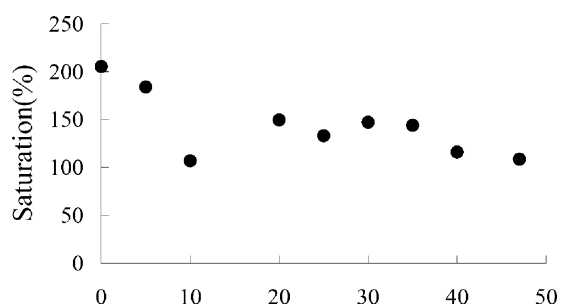
Fig. 19. Longitudinal distribution of methane saturation ratio in South Pacific.

kg^{-1} at 0° and 5°S as compared with those in the bulk of mixed layer. *Watanabe et al.* [1995] reported that the saturation ration ranged from 109-162% in the North Pacific (0-40°N along 165° E). In the western Equatorial Pacific, where is the area known as the western Pacific warm pool with low macro-nutrients and low salinity, they reported lower methane concentration (~2.5 nmol kg^{-1}). The relatively high methane concentration in the present work is likely to be associated with high biological activity and methane production due to the equatorial upwelling. The saturation ratio became lowest near 10°S, and gradually increase with going to the south (Fig. 20). This is the pattern similar to that observed by *Bates* [1996] and *Kelley and Jeffrey* [2002].

The maximum concentration of methane in the subsurface layer or in the mixed layer was within the range from 2.9 to 4 nmol kg^{-1} along 160°W (Fig. 20). The vertical distribution of methane concentration differed from those of biological parameters such as chlorophyll *a*, macronutrients, and so on. This was mainly caused by processes of methane production in seawater as mentioned above. *Kelley and Jeffrey* [2001] observed subsurface maxing, generally at the base
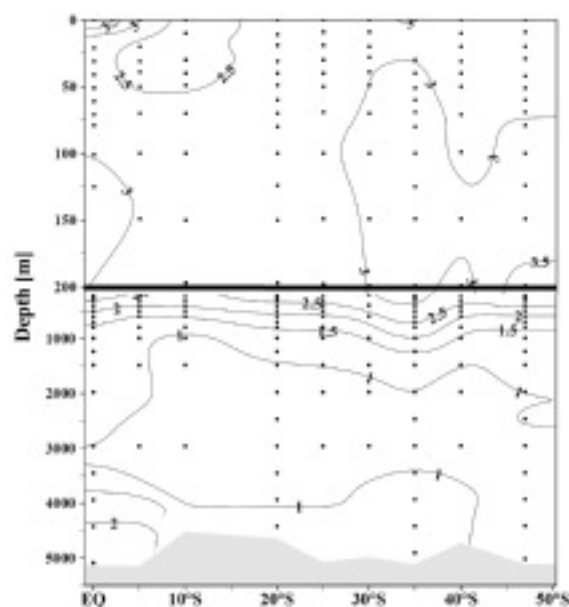
Fig. 20. Distribution of methane concentration in the South Pacific (nmol kg^{-1}). Note the change in scales for surface 200 m. The numeral of most upper shows the methane saturation ratio (%).

of the thermocline, in dissolved methane concentration at every site along the transect. However, our results sometimes showed no clear maximum concentration of methane in the subsurface layer.

3.3.1.2 The increase in the marine surface methane for past of 30 years

Bange et al. [1994] examined diurnal variation in oceanic methane in the south central North Sea, and found little change. Until now, there are only a few works which focused on seasonal and year-to-year change in oceanic methane. The observation of the surface water methane in the ocean was carried out in the beginning in 1970's, and its saturation ratio of 130% was reported [*Ehhalt*, 1974]. Atmospheric methane concentration in those days was ~1.4 ppmv, methane concentration in the air in equilibrium to the surface water in oceanic region was ~1.8 ppmv. In this study, the saturation ratio is calculated as the atmospheric methane concentration is to be 1.8 ppmv. The saturation ratio shown here had over 100% (supersaturated), and the possibility was shown in which methane concentration of the surface water has increased over years in response to the increase of atmospheric methane.

3.3.2 Methane in the Southern Ocean
3.3.2.1 Oceanic structure in the Southern Ocean

In the Southern Ocean, major fronts were confirmed [*Preliminary Report of The Hakuho Maru Cruise KH-01-3,* 2003; *Preliminary Report on the 43rd Japanese Antarctic Research Expedition Marine Science Cruise by Research Vessel Tangaroa,* 2002] in January 2002 (Fig. 21) and in February 2002 (Fig. 22). Figs. 21 and 22 show that the each oceanic structure has not largely changed during the period from January 2002 to February 2002.

Around 49° to 49.5°S, a steep horizontal gradient in surface temperature (Fig. 21) and salinity was observed (data not shown) in January 2002. This was recognized as the Subantarctic Front, which is generally defined by the maximum temperature gradient in the range 3° to 8°C at 100 to 400 m
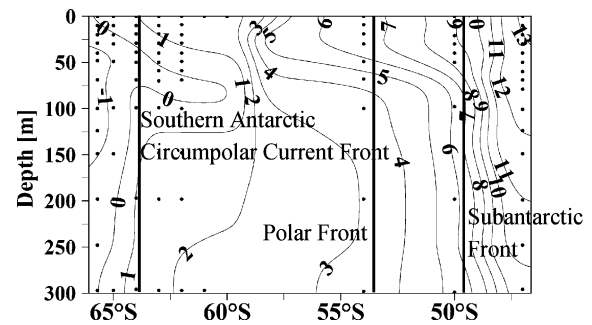

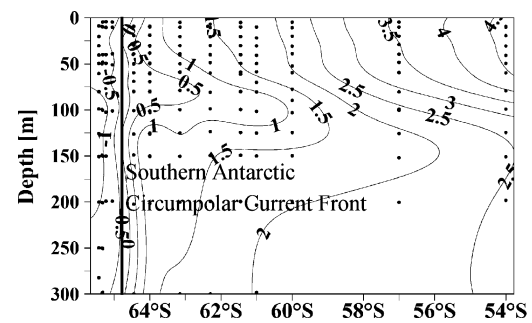Fig. 21. Distribution of temperature in January.

Fig. 22. Distribution of temperature in February.

depth [*Belkin and Gordon*, 1996]. The Polar Front is commonly defined as the northernmost extent of temperature minimum water with temperatures less than 2°C at 200 m depth [*Belkin and Cordon*, 1996]. During our cruise, these features were recognized around 54°S. South of the Polar Front, cold fresh surface waters are known as Antarctic Surface Water.

Orsi et al. [1995] identified another deep front south of the Polar Front that coincides with the southern limit of temperature maximum water warmer than 1.8°C and is known as the Southern Antarctic Circumpolar Current Front. *Rintoul and Bullister* [1999] found this front to be about 63°S along 140°E, corresponding to the southernmost maximum of eastward transport. The existence of the Southern Antarctic Circumpolar Current Front in January and February was around 63° and 65°S respectively. An upwelling of water with warmer temperature (>1°C) and higher salinity (34.5) was observed around 64°S, probably forming the Antarctic Divergence.

The Permanently Open Ocean Zone (POOZ) is commonly defined by waters between the Polar Front and the Southern Antarctic Circumpolar

Current Front. South of the Southern Antarctic Circumpolar Current Front, where are known as Seasonal Ice Zone (SIZ). In this paper, it mainly argues in north and south in the Southern Antarctic Circumpolar Current Front (i.e. POOZ and SIZ), because there is no data from 54°S to the north in the observation in February.

Antarctic Bottom Water is a dense water mass that forms around some areas of the Antarctic coast and sinks to abyssal depths along the Antarctic continental slope [*Orsi et al.*, 1999]. *Rintoul and Bullister* [1999] showed that Antarctic Bottom Water along 140°E was rich in CFCs at depths of >3000 m. The high concentrations of CFCs found in Antarctic Bottom Water suggested that production and export of Antarctic Bottom Water is an efficient mechanism for transporting surface waters to the deep sea.

3.3.2.2 High methane concentration in the surface layer

We divided the area south of the Polar Front into two zones, POOZ and SIZ. In the former zone, the maximum methane concentrations were observed in the mixed layer and they are almost the same value of 3.7 ± 0.6 nmol kg^{-1} (Figs. 23–25). In the latter zone, the maximum methane concentration was also observed in the mixed layer, and methane concentration was apparently associated with chlorophyll a concentration (Figs. 26 and 27). Concentration of chlorophyll a is controlled by photosynthetic process and zooplankton grazing and degradation of the organic matter [*Oudot et al.*, 2002]. As mentioned above methane is produced by methanogenic bacteria and meth-
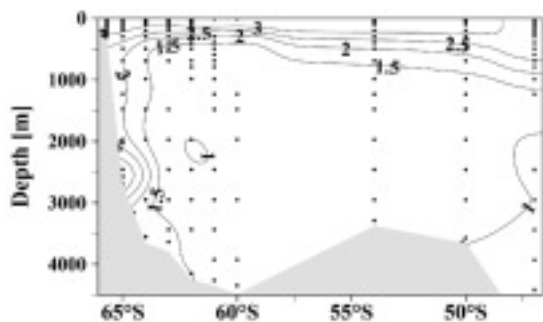
anogen associated with suspended particles, fecal pellets, and guts of zooplankton. The relationship between methane concentration and quantity/grazing rate of zooplankton should be considered, because the phytoplankton does not form the methane directly. Unfortunately, at present data of the zooplankton are not available.
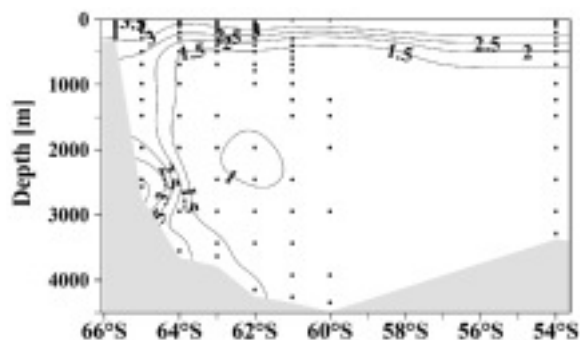

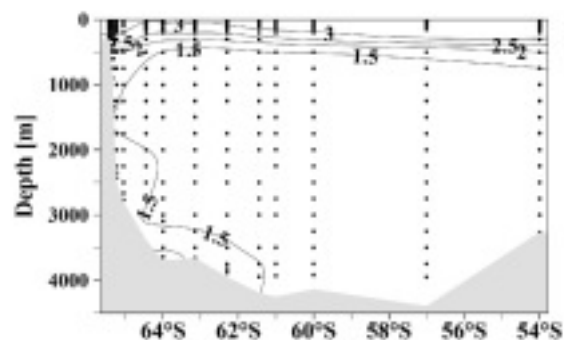**Fig. 24.** As for Figure 23 except in from 54° to 66°S.

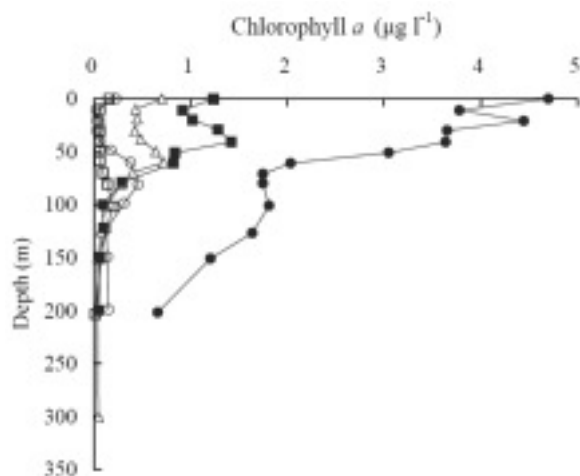**Fig. 25.** Distribution of methane concentration in February from 54° to 66°S (nmol kg^{-1}).

Fig. 26. Vertical profiles of chlorophyll *a* concentration upper 350 m. Square and diamond represent the data in January and February respectively.

Fig. 23. Distribution of methane concentration in January from 43° to 66°S (nmol kg^{-1}).
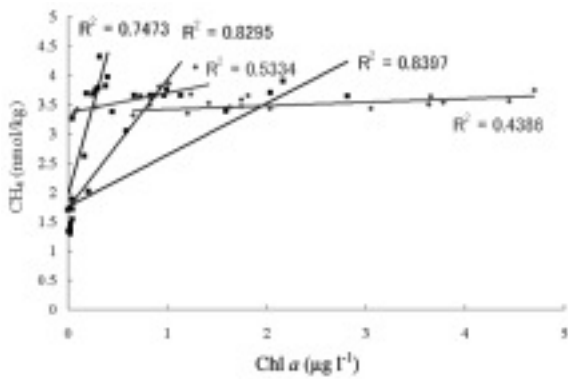
Fig. 27. Methane concentration vs. chlorophyll *a* from 62°S to 64°S. Blue square and red diamond represent the data in January and February respectively.

In the POOZ and SIZ, the methane concentration below the mixed layer decreased drastically to the level of 1 nmol kg⁻¹ (Figs. 23-25), therefore we did not found any subsurface maximum methane concentrations south of the Polar Front. *Holmes et al.* [2000] suggested methane production in organic rich particles at the pycnocline to account for the subsurface maximum. Taking into discussions about methane production and oxidation [*Holmes et al.*, 2000; *Ward and Kilpatrick*, 1993; *Karl and Tilbrook*, 1994], we examined the vertical profiles of methane concentration at ~27.1 σ_θ which is the density at the base of mixed layer in south of the Polar Front (Fig. 28). Around this $\sigma\theta$ the methane concentration changed steeply at every site along the transects. This support the mechanism suggested by *Holmes et al.* [2000].

3.3.2.3 Methane saturation and sea-air flux
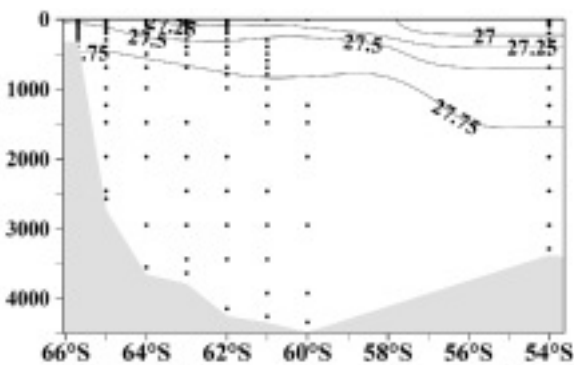
The methane saturation ratio was shown in Figs. 29 and 30 in the each station. In the observation in January, all the station was supersaturated, and the methane discharged to the atmosphere from the ocean, and in the observation in February, some station was undersaturation, and it seemed to absorb methane from the atmosphere.

The flux in the observation in January was calculated by using equation (1), (2), and (4). The wind speed was the average wind speed measured by the ship's anemometer during the sampling period. The high rate flux was observed in the station where a good correlation between chlorophyll a concentration and methane concentration.

As mentioned in 3.3, the relative error associated with kw determined by equation (4) is about 25%, assuming a 10% error on the Schmidt number [*Wanninkhof*, 1992] and using the measured variability in the wind speeds while sampling. About 40% error is contained as a whole.
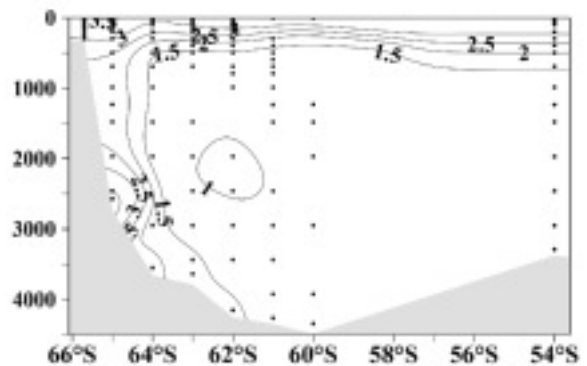

Fig. 29. Methane saturation ratio (%) with distribution in January.
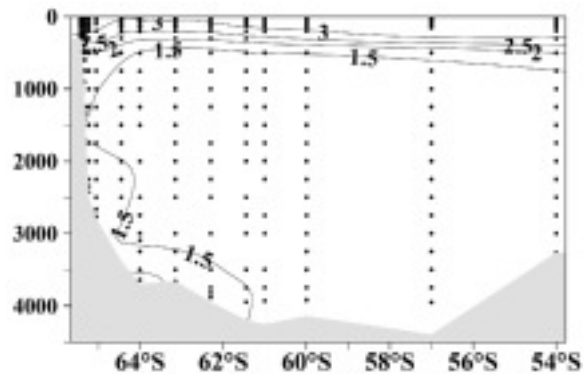

Fig. 28. Distribution of σ_θ in January.

Fig. 30. As for Figure 29 except in February.

3.3.3 Summary

In January and February 2002, measurement oceanic methane were made in the South Pacific (0° to 47°S along 160°W), and in the Southern Ocean (47° to 66°S along 140°E), the equatorial region showed higher saturation ratio of methane,

205% at 0° and 184% at 5°. This high saturation ratio was probably caused by the high biological activity and methane production due to equatorial upwelling. The saturation ratio became low near 10°S (107%) and gradually increased toward south in the South Pacific. The maximum concentration of methane in the subsurface or in the surface ranged from 2.8 to 4.7 nmol kg⁻¹.

In the Southern Ocean the maximum concentration of methane was found in the mixed layer. And methane concentration below the mixed layer decreased drastically to the level of 1 nmol kg⁻¹. This vertical profile of methane is markedly deferent from those in lower latitudes. In
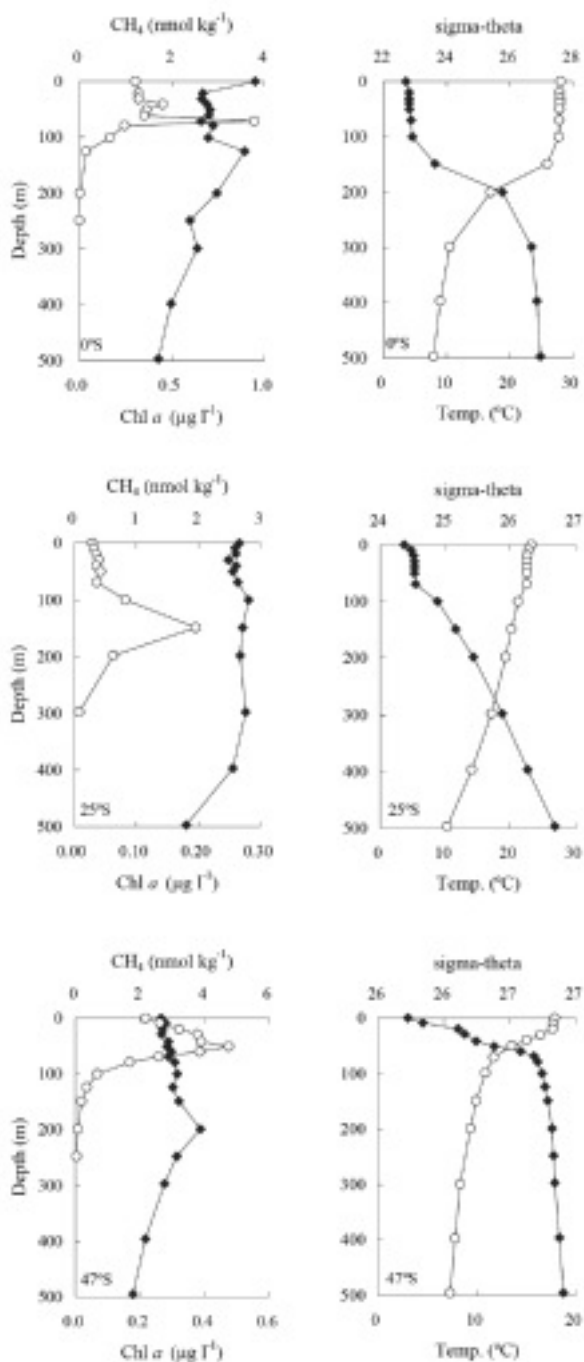

Fig. 31. Vertical distribution of methane concentration, Chlorophyll *a* concentration, Sigma-theta, and Water temperature in January 2002.
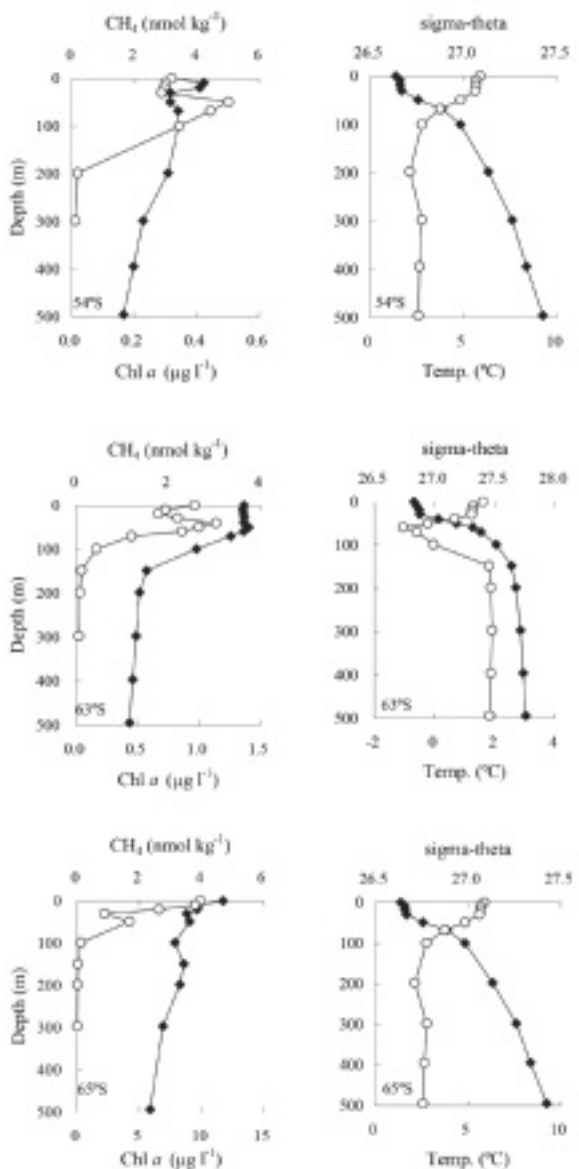
Fig. 31. (Continued)

the SIZ, we found the good correlation between methane and chlorophyll a concentrations. Because the phytoplankton does not form the methane directly, the data of zooplankton such as biomass and grazing rate are necessary to examine the factor which controls the vertical distribution of the methane. However at the present, zooplankton data are not available. The vertical profiles of methane suggest the importance of in situ methane production in organic rich particles at about 27.1 σ_θ.

Chapter 4   Global estimates of oceanic methane and General outlook

4.1   Global estimates of oceanic methane

In chapter 2, I described the observations in detail in the Western part of the Sea of Okhotsk in which the observation was done only in the limited area in the previous study, and the fluxes were estimated according to the area of the different methane generation mechanism. It was found that the methane concentration in the surface layer is low due to the strong stratification while the anomalously high methane concentration is observed near bottom at the shelfbreak, and the flux is high by the tidal mixing close to the shore. The concentration of methane was used as a chemical tracer and methane oxidation rate in an extremely high methane concentration area was estimated.

In chapter 3, features of the spatial distribution in South Pacific were clarified, and the concentration-change of the methane in the surface ocean was indicated. I observed methane in detail temporally in the Southern Ocean which has few data of methane in the previous study, and clarified the concentration was the highest in the surface. The existence of methane generation process through the phytoplankton-zooplankton was indicated because of the high correlation with the chlorophyll a.

The global fluxes of the methane to the atmosphere are calculated on the basis of the saturation ratio of the North and South Pacific and the Southern Ocean to evaluate the role of the high latitude ocean; the Sea of Okhotsk and the Southern Ocean.

4.2   Methane in the high latitude ocean

In the high latitude ocean of the Sea of Okhotsk and the Southern Ocean, the average surface methane concentration was estimated to be 3.5 $\pm$ 0.4 nmol kg^{-1} and 3.6 $\pm$ 0.4 nmol kg^{-1} (in January) and 3.6 $\pm$ 0.1 nmol kg^{-1} (in February) respectively. In the low latitude ocean of North Pacific and South Pacific, the average surface methane concentration was estimated to be 2.4 $\pm$ 0.2 nmol kg^{-1} [*Watanabe et al.*, 1995] and 2.9 $\pm$ 0.5 nmol kg^{-1} respectively. The surface methane concentration in the high latitude ocean is higher than that of the low latitude. However as reported the saturation ratio of the methane has been estimated with the value which slightly exceeds 100% and there is no seasonal variation [*Bates et al.*, 1996].

4.3   Comparison with sea-air flux

The degree of saturation and air-sea exchange flux of methane were calculated by equations (1) and (2). The wind speed used in this work was the average by the ship's anemometer during the sampling periods of observations. Therefore we calculated the kw by equation (4) [*Wanninkhof*, 1992],

$$k_w = 0.31 v^2 \left(\frac{Sc}{660}\right)^{-\frac{1}{2}} \qquad (4)$$

where Sc is the Schmidt number of methane, which is defined as the ratio of the kinematic viscosity of water to the diffusion coefficient of methane. By using equations (2) and (4), we calculated the methane fluxes at in situ water temperature, salinity. The average methane flux of Southern Ocean in January and February was 2.6 mol km^{-2} d^{-1} and 0.6 mol km^{-2} d^{-1} respectively and that of the Sea of Okhotsk was 3.1 mol km^{-2} d^{-1}.

The saturation ratio of methane reported here is generally within the values in the open ocean reported earlier. In February 2002, surface methane concentration in the Southern Ocean was occasionally undersaturated with respect to the atmospheric equilibrium. Similar undersaturation has been observed in southern high latitudes in previous studies [*Bates et al.*, 1996; *Kelley and Jeffrey*, 2002]. High saturation ratio was found

in the equatorial Pacific as described above.

The flux of methane between the sea and the air was calculated by equations (2) and (4). The flux of methane between the sea and air ranged from -0.1 to 11.1 mol CH_4 km^{-2} d^{-1}, from the sites of two transects (Table 5 and Fig. 32). The negative fluxes indicate the flux of methane from atmosphere into the ocean. The average flux obtained in this work was 3.4 ± 1.8 mol CH_4 km^{-2} d^{-1} south of 15°S and 6.9 ± 5.5 mol CH_4 km^{-2} d^{-1} in the equatorial Pacific.

The data along two transects were binned into zones on the basis of *Bates et al.* [1996]. These zones were chosen to bound the major oceanographic features of the Pacific (Table 5). In order to estimate the methane flux between sea and air, we use the data of *Watanabe et al.* [1995] in the northern hemisphere. In the equatorial Pacific,

Watanabe et al. [1995] reported lower flux of methane of 1 mol CH_4 km^{-2} d^{-1}, which was methane flux in the oligotrophic surface water of the western Pacific warm pool. We estimated methane flux in the two regions of the equatorial Pacific; the warm pool to the west and the Pacific equatorial divergence [*Le Borgne et al.*, 2002].

Regional methane emissions ranged from 0.1 to 1.3 Tg CH_4 y^{-1}. The emissions in the Southern Hemisphere are about 82% of the total. Although our estimates is based on a limited number of data, the estimated methane emission is similar to the open ocean flux determined by *Bange et al.* [1994], and an order of magnitude larger than *Bates et al.* [1996] and *Kelly and Jeffrey* [2002]. According to *Bange et al.* [1994] and *Lambert and Schmidt* [1993], approximately 25-40% of the total oceanic methane fluxes come

Table 5. Regional emission of CH_4 from the Ocean to the Atmosphere.

Region	Flux mol CH_4 km^{-2} d^{-1}		Area 10^6 km^2	emission rate Tg CH_4 y^{-1}	
North of 45°N	1.6		35.7	0.3	
30°-45°N*	0.9		28.3	0.1	
15°-30°N*	1.3		40.9	0.3	
0°-15°N*	1.0		49.8	0.3	
0°-15°S†	6.9 (1.0)		50.4	1.0	
15°-30°S	4.5		47.6	1.3	
30°-45°S	2.3		53.6	0.7	
45°-60°S	2.4	1.2‡	34.6	0.5	0.2
South of 60°S	2.8	0.4‡	20.2	0.3	0.0
			Total	4.9	4.3

Watanabe et al. [1996]

†The Pacific equatorial divergence was assumed to be in the area between 80°W and 170°E. The remaining area was assumed to be equal to 1 mol CH_4 km^{-4} d^{-1}.

‡based on observations in February
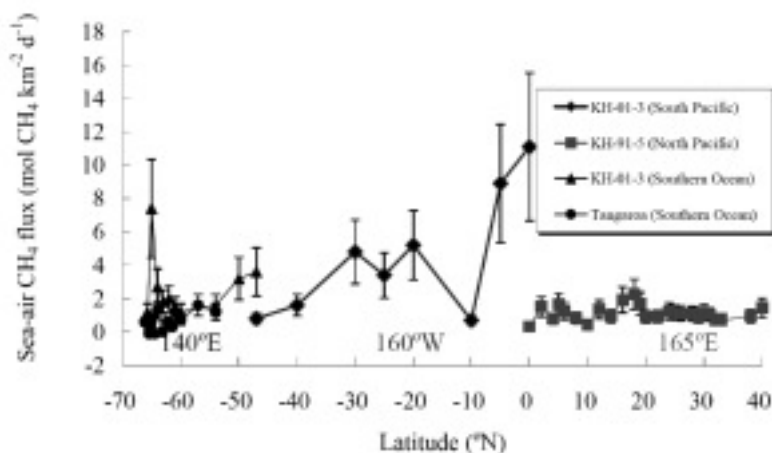
Fig. 32. Longitudinal distribution of sea-air CH_4 flux.

from open ocean.

4.4 General Outlook

Information of the methane isotope is necessary to understand the methane production and/or consumption process in the ocean more in detail. In the Southern Ocean, the undersaturated methane in the surface layer with respect to the atmospheric equilibrium suggested the necessity of the seasonally detailed observation. In order to grasp the biogeochemical dynamic of methane through the ocean — atmosphere, observation must be done in detail temporally and spatially.

References

Alldredge, A. A., Cohen, Y., Can microscale chemical patches persist in the sea? Microelectrode study of marine snow, fecal pellets, Science, 235, 689–691, 1987.

Bange, H. W., U. H. Bartell, S. Rapsomanikis, and M. O. Andreae, Methane in the Baltic and the North seas and a reassessment of the marine emissions of methane, *Global Biogeochem. Cycles*, 8, 465–480, 1994.

Bange, H. W., S. Dahlke, R. Ramesh, L.-A. Meyer-Reil, S. Rapsomanikis, and M. O. Andreae, Seasonal study of methane and nitrous oxide in the coastal waters of the southern Baltic Sea, *Estu. Coast. Shelf Sci.*, 47, 807–817, 1998.

Bekki, S., K. S. Law and J. A. Pyle, Effect of ozone depletion on atmospheric CH_4 and CO concentrations. *Nature*, 371, 595–597, 1994.

Blunier, T., J. Chappellaz, J. Schwander, J.-M. Barnola, T. Desperts, B. Stauffer and D. Raynaud, Atmospheric methane, record from a Greenland ice core over the last 1000 years. *J. Geophys. Res.*, 20, 2219–2222, 1993.

Blunier, T., J. Chappellaz, J. Schwander, B. Stauffer and D. Raynaud, Variations in atmospheric methane concentration during the Holocene epoch, *Nature*, 374, 46–49, 1995.

Brook, E. J., S. Harder, J. Severinghaus, E. J. Steig and C. M. Sucher, On the origin and timing of rapid changes in atmospheric methane during the last glacial period. *Global Biogeochem. Cycles*, 14, 559–572, 2000.

Burke, R. A., Jr., D. F. Reid, J. M. Brooks, and D. M. Lavoie, Upper water column methane geochemistry in the eastern tropical North Pacific, *Limnol. Oceanogr.*, 28, 19–32, 1983.

Cicerone, R. J., and R. S. Oremland, Biogeochemical aspects of atmospheric methane, *Global Biogeochem. Cycles*, 2, 299–327, 1988.

Chappellaz, J., T. Blunier, S. Kints, A. Dällenbach,

J. -M. Barnola, J. Schwander, D. Raynaud and B. Stauffer, Changes in the atmospheric CH$_4$ gradient between Greenland and Antarctica during the Holocene. *J. Geophys. Res.*, 102, 15987–15999, 1997.

Conrad, R., and W. Seiler, Methane and hydrogen in seawater (Atlantic Ocean), *Deep-Sea Res.*, 35, 1903–1917, 1988.

Cranston, R. E., G. D. Ginsburg, V. A. Soloviev, and T. D. Lorenson, Gas venting and hydrate deposits in the Okhotsk Sea, *Bull. Geol. Soc. Den.*, 41, 80–85, 1994.

de Angelis, M. A., and C. Lee, Methane production during zooplankton grazing on marine phytoplankton, *Limnol. Oceanogr.*, 39, 1298–1308, 1994.

Dickens, G. R., The blast in the past. *Nature*, 401, 752–755, 1999.

Dickens, G., On the fate of past gas: what happens to methane released from a bacterially mediated gas hydrate capacitor? *Geochem. Geophys. Geosyst.*, 2, 2000GC000131, 2001.

Ding, A. and M. X. Wang, A Model for methane emission from rice field and its application in southern China. *Advances in Atmospheric Sci.*, 13, 159–168, 1996.

Dlugokencky, E. J., E. G. Dutton, P. C. Novelli, P. P. Tans, K. A. Masarie, K. O. Lantz and S. Madronich, Changes in CH$_4$ and CO growth rates after the eruption of Mt. Pinatubo and their link with changes in tropical tropospheric UV flux. *Geophys. Res. Lett.*, 23, 2761–2764, 1996.

Dlugokencky, E. J., K. A. Masarie, P. M. Lang and P. P. Tans, Continuing decline in the growth rate of the atmospheric methane burden. *Nature*, 393, 447–450, 1998.

Ehhalt, D. H., The atmospheric cycle of methane, *Tellus*, 26, 58–70, 1974.

Etheridge, D. M., L. P. Steele, R. J. Francey and R. L. Langenfelds, Atmospheric methane between 1000 A. D. and present: Evidence of anthropogenic emissions and climatic variability. *J. Geophys. Res.*, 103, 15979–15993, 1998.

Francey, R. J., M. R. Manning, C. E. Allison, S. A. Coram, D. M. Etheridge, R. L. Langenfelds, D. C. Lowe and L. P. Steele, A history of δ^{13}C in atmospheric CH$_4$ from the Cape Grim air archive and Antarctic firn air. *J. Geophys. Res.*, 104, 23631–23643, 1999.

Fuglestvedt, J. S., J. E. Jonson and I. S. A. Isaksen, Effects of reduction in stratospheric ozone on tropospheric chemistry through changes in photolysis rates. *Tellus*, 46B, 172–192, 1994.

GANAL, 18–L global analysis monthly tape data set: monthly tape for GL-objective analysis data set on lat-lon grid and GL-spectral model with complete physics, pp. 1–2, Japan Meteorological Agency, Tokyo, 1998, 1999, 2000.

Geodekyan, A. A., V. Ya. Trotsyuk, and Z. I. Verkshovskaya, Hydrocarbon gases in bottom sediment of the Sea of Okhotsk (in Russian), *Dokl. Akad. Nauk* SSSR, 226, 228–230, 1976.

Ginsburg, G. D., V. A. Soloview, R. E. Cranston, T. D. Lorenson, and K. A. Kvenvolden, Gas hydrates from the continental slope, offshore Sakhalin Island, Okhotsk Sea, *Geo Mar. Lett.*, 13, 41–48, 1993.

Gornitz, V., and I. Fung, Potential distribution of methane hydrates in the world's oceans, *Global Biogeochem. Cycles*, 8, 335–347, 1994.

Hein, R., P. J. Crutzen and M. Heinmann, An inverse modeling approach to investigate the global atmospheric methane cycle. *Global Biogeochem. Cycles*, 11, 43–76, 1997.

Hogan, K. B. and R. C. Harriss, Comment on 'A dramatic decrease in the growth rate of atmospheric methane in the northern hemisphere during 1992' by Dlugokencky et al. *Geophys. Res. Lett.*, 21, 2445–2446, 1994.

Holmes, M. E., F. J. Sansone, T. M. Rust, and B. N. Popp, Methane production, consumption, and air-sea exchange in the open ocean: An evaluation based on carbon isotopic ratios, *Global Biogeochem. Cycles*, 14, 1–10, 2000.

Houweling, S., T. Kaminski, F. Dentener, J. Lelieveld and M. Heimann, Inverse modeling of methane sources and sinks using the adjoint of a global transport model. *J. Geophys. Res.*, 104, 26137–26160, 1999.

IPCC (Intergovernmental Panel on Climate Change), *Climate Change 1995*, in The Science of Climate Change, edited by J. T.

Houghton, L. G. M. Filho, B. A. Callander, N. Harris, A. Kattenberg, and K. Maskell, Cambridge Univ. Press, New York, 572 pp. 1996.

IPCC, Climate Change 2001, The Scientific Basis, edited by J. T. Houghton, Y. Ding, D. J. Griggs, M. Noguer, P. J. van der Linden, X. Dai, K. Maskell, and C. A. Johnson, Cambridge Univ. Press, New York, 882 pp. 2001.

Itoh, M. and K. I. Ohshima, Seasonal variation of water masses and sea level in the southwestern part of the Okhotsk Sea, *J. Oceanogr.*, 56, 643–654, 2000.

Jayakumar, D. A., S. W. A. Naqvi, P. V. Narvekar, and N. D. George, Methane in coastal offshore waters of the Arabian Sea, *Mar. Chem.*, 74, 1–13, 2001.

Jones, R. D., Carbon monoxide and methane distribution and consumption in the photic zone of the Sargasso Sea, *Deep-Sea Res.*, 38, 625–635, 1991.

Karl, D. M., and B. D. Tilbrook, Production and transport of methane in oceanic particulate organic matter, *Nature*, 368, 732–734, 1994.

Karlsdottir, S. and I. S. A. Isaksen, Changing methane lifetime: Possible cause for reduced growth. *Geophys. Res. Lett.*, 27, 93–96, 2000.

Kennett, J. P., K. G. Cannariato, I. L. Hendy and R. J. Behl, Carbon isotopic evidence for methane hydrate instability during quaternary interstadials. *Science*, 288, 128–133, 2000.

Kiene, R. P., Production and consumption of methane in aquatic system, in *Microbial Production and Consumption of Greenhouse Gases*, edited by J. E. Rogers and W. B. Whitman, pp. 39–55, American Society of Microbiology, Washington, 1992.

Kitani, K., An oceanographic study of the Okhotsk Sea: particularly in regard to cold waters, *Bull. Far Seas. Fish. Res. Lab.*, 9, 45–77, 1973.

Krol, M., P. J. Van Leeuwen and J. Lelieveld, Global OH trend inferred from methylchloroform measurements. *J. Geophys. Res.*, 103, 10697–10711, 1998.

Kvenvolden, K. A., M. D. Lilley, T. D. Lorenson, P. W. Barnes, and E. McLaughlin, The Beaufort Sea continental shelf as a seasonal source of atmospheric methane, *Geophys. Res.*

Lett., 20, 2459–2462, 1993.

Lammers, S., E. Suess, M. N. Mansurov, and V. V. Anikiev, Variation of atmospheric methane supply from the Sea of Okhotsk induced by the seasonal ice cover, *Global Biogeochem. Cycles*, 9, 351–358, 1995.

Lassey, K. R., D. C. Lowe, C. A. M. Brenninkmeijer and A. J. Gomez, Atmospheric methane and its carbon isotopes in the southern hemisphere: Their time series and an instructive model. Chemosphere: *Global Change Sci.*, 26, 95–100, 1993.

Le Borgne, R, R. T. Barber, T. Delcroix, H. Y. Inoue, D. J. Mackey, and M. Rodier, Pacific warm pool and divergence: temporal and zonal variations on the equator and their effects on the biological pump. *Deep-Sea Res.*, 49, 2471–2512, 2002.

Lowe, D. C., C. A. M. Brenninkmeijer, G. W. Brailsford, K. R. Lassey and A. J. Gomez, Concentration and 13C records of atmospheric methane in New Zealand and Antarctica: Evidence for changes in methane sources. *J. Geophys. Res.*, 99, 16913–16925, 1994.

Lowe, D. C., M. R. Manning, G. W. Brailsford and A. M. Bromley, The 1991–1992 atmospheric methane anomaly: Southern Hemisphere C-13 decrease and growth rate fluctuations. *Geophys. Res. Lett.*, 24, 857–860, 1997.

Mak, J. E., M. R. Manning and D. C. Lowe, Aircraft observations of delta C-13 of atmospheric methane over the Pacific in August 1991 and 1993: Evidence of an enrichment in (CH_4)-C-13 in the Southern Hemisphere. *J. Geophys. Res.*, 105, 1329–1335, 2000.

McNeil, B. I., B. Tilbrook, and R. J. Matear, Accumulation and uptake of anthropogenic $CO2$ in the Southern Ocean, south of Australia between 1968 and 1996. *J. Geophys. Res.*, 106, 31, 431–31, 445, 2001.

Mizuta, G., Y. Fukamachi, K. I. Ohshima and M. Wakatsuchi, Structure and seasonal variability of the East Sakhalin Current, *J. Phys. Oceanogr.*, 2003 in press.

Nakamura, T., Y. Nojiri, A. Otsuki, and S. Hashimoto, Methane concentration and its variation in seawater of highly eutrophic Tokyo

Bay (in Japanese with English abstract), *Geochemistry* 28, 47-57, 1994.

Neue, H. -U. and R. Sass, The budget of methane from rice fields. IGACtivities *Newsletter*, 12, 3-11, 1998.

Norris, R. D. and U. Röhl, Carbon cycling and chronology of climate warming during the Palaeocene/Eocene transition. *Nature*, 401, 775-778, 1999.

Ohshima, K. I., M. Wakatsuchi, Y. Fukamachi, and G. Mizuta, Near-surface circulation and tidal currents of the Okhotsk Sea observed with satellite-tracked drifters, *J. Geophys. Res.*, 107, 3195, doi: 10.1029/2001JC001005, 2002.

Orsi, A. H., G. C. Johnston, and J. L. Bullister, Circulation, mixing and production of Antarctic Bottom Water, *Progress in Oceanogr.*, 43, 55-109, 1999.

Owens, N. J. P., C. S. Law, R. F. C. Mantoura, P. H. Burkill, and C. A. Llewellyn, Methane flux to the atmosphere from the Arabian Sea, *Nature*, 354, 293-296, 1991.

Petit, J. R., J. Jouzel, D. Raynaud, N. I. Barkov, J. M. Barnola, I. Basile, M. Bender, J. Chappellaz, Davis, G. Delaygue, M. Delmotte, V. M. Kotlyakov, M. Legrand, V. Y. Lipenkov, C. Lorius, L. Pepin, C. Ritz, E. Saltzman and M. Stievenard, Climate and atmospheric history of the past 420,000 years from the Vostok ice core, Antarctica. *Nature*, 399, 429-436, 1999.

Preliminary Report of The Hakuho Maru Cruise KH-01-3, edited by M. Terazaki, H. Ogawa, and K. Tamaki, Ocean Research Institute, Univ. of Tokyo, 170 pp. 2003.

Preliminary Report on the 43rd Japanese Antarctic Research Expedition Marine Science Cruise by Research Vessel Tangaroa, edited by T. Odate, National Institute of Polar Research, Tokyo, 69 pp. 2002.

Prinn, R. G., R. F. Weiss, B. R. Miller, J. Huang, F. N. Alyea, D. M. Cunnold, P. J. Fraser, D. E. Hartley and P. G. Simmonds, 285 Atmospheric Chemistry and Greenhouse Gases Atmospheric trend and lifetime of CH_3CCl_3 and global OH concentrations. *Science*, 269, 187-192, 1995.

Quay, P. D., S. L. King, J. Stutsman, D. O. Wilbur, L. P. Steele, I. Fung, R. H. Gammon, T. A. Brown, G. W. Farwell, P. M. Grootes and F. H. Schmidt, Carbon isotopic composition of atmospheric CH_4: Fossil and biomass burning source components. *Global Biogeochem. Cycles*, 5, 25-47, 1991.

Quay, P., J. Stutsman, D. Wilbur, A. Stover, E. Dlugokencky and T. Brown, The isotopic composition of atmospheric methane. *Global Biogeochem. Cycles*, 13, 445-461, 1999.

Rehder, G., R. W. Collier, K. Heeschen, P. M. Kosro, J. Barth, and E. Suess, Enhanced marine CH_4 emissions to the atmosphere off Oregon caused by coastal upwelling, *Global Biogeochem. Cycles*, 16, 10.1029/2000GB001391, 2002.

Ridgwell, A. J., S. J. Marshall and K. Gregson, Consumption of methane by soils: A process-based model. *Global Biogeochem. Cycles*, 13, 59-70, 1999.

Rintoul, S. R. and J. l. Bullister, A lake Winter Hydrographic Section from Tasmania to Antarctica, *Deep-Sea Res.*, 46, 1417-1454, 1999.

Sass, R. L., F. M. Fisher Jr., A. Ding and Y. Huang, Exchange of methane from rice fields: national, regional, and global budgets. *J. Geophys. Res.*, 104, 26943-26951, 1999.

Schlitzer, R., Ocean Data View, http://www.awi-bremerhaven.de/GEO/ODV, 2002.

Scranton, M. I. and P. G. Brewer, Occurrence of methane in the near-surface waters of the western subtropic North-Atlantic. *Deep-Sea Res.*, 24, 127-138, 1977.

Singh, H. B., A. N. Thakur, Y. E. Chen and M. Kanakidou, Tetrachloroethylene as an indicator of low Cl atom concentrations in the troposphere. *Geophys. Res. Lett.*, 23, 1529-1532, 1996.

Stauffer, B., G. Fischer, A. Neftel and H. Oeschger, Increase of atmospheric methane recorded in Antarctic ice core, Science, 229, 286 *Atmospheric Chemistry and Greenhouse Gases* 1386-1388, 1985.

Stevens, C. M. and A. Engelkemeir, Stable carbon isotopic composition of methane from some natural and anthropogenic sources. *J. Geo-*

phys. Res., 93, 725-733, 1988.

Suess, E., G. Bohrmann, J. Greinert and E. Lausch, Flammable ice. *Scientific American*, 52-59/ 76-83, 1999.

Talley L. D., Okhotsk Sea water anomaly: implications for ventilation in the North Pacific, *Deep-Sea Res.*, 38, Suppl. 1, 171-190, 1991.

Tans, P. P., P. S. Bakwin, L. Bruhwiler, T. J. Conway, E. J. Dlugokencky, D. W. Guenther, D. R. Kitzis, P. M. Lang, K. A. Masarie, J. B. Miller, P. C. Novelli, K. W. Thoning, B. H. Vaughn, J. W. C. White, and C. Zhao, Carbon cycle, in Climate Monitoring and Diagnostics Laboratory Summary Report No. 26, edited by D. B. King and R. C. Schnell, pp. 28-50, US Department of Commerce, Washington, 2002.

Tilbrook, B. D., and D. M. Karl, Methane sources, distributions and sinks from California coastal waters to the oligotrophic North Pacific gyre, *Mar. Chem.*, 49, 51-64, 1995.

Tsurushima, N., S. Watanabe, N. Higashitani, and S. Tsunogai, Methane in the East China Sea water, *J. Oceanogr.*, 52, 221-233, 1996.

Valentine, D. L., D. C. Blanton, W. S. Reeburgh, and M. Kastner, Water column methane oxidation adjacent to an area of active hydrate dissociation, Eel River Basin, *Geochim. Cosmochim. Acta*, 65, 2633-2640, 2001.

Wahlen, M., N. Tanaka, R. Henery, B. Deck, J. Zeglen, J. S. Vogel, J. Southon, A. Shemesh, R. Fairbanks and W. Broecker, Carbon-14 in methane sources and in atmospheric methane: The contribution of fossil carbon. *Science*, 245, 286-290, 1989.

Wang, M. X. and X. Shangguan, CH$_4$ emission from various rice fields in P. R. China. *Theoretical and Applied Climatology*, 55, 129-138, 1996.

Wanninkhof, R., Relationship between wind speed and gas exchange over the ocean, *J. Geophys Res.*, 97, 7373-7382, 1992.

Ward, B. B., K. A. Kilpatrick, P. C. Novelli, and M. I. Scranton, Methane oxidation and methane fluxes in the ocean surface layer and deep anoxic waters, *Nature*, 327, 226-229, 1987.

Watanabe, S., N. Higashitani, N. Tsurushima, and S. Tsunogai, Annual Variation of methane in seawater in Funka Bay, Japan. *J. Oceanogr.*, 50, 415-421, 1994.

Watanabe, S., N. Higashitani, N. Tsurushima, and S. Tsunogai, Methane in the western North Pacific, *J. Oceanogr.*, 51, 39-60, 1995.

Wiesenburg, D. A., and N. L. Guinasso, Jr., Equilibrium solubilities of methane, carbon monoxide, and hydrogen in water and sea water, *J. Chem. Eng. Data*, 24, 356-360, 1979.

Yamamoto, M, S. Watanabe, S. Tsunogai, and M. Wakatsuchi, Effects of sea ice formation and diapycnal mixing on the Okhotsk Sea intermediate water clarified with oxygen isotopes, *Deep Sea Res.*, 102, 893-909, 2002.

Yasuda, I., The origin of the North Pacific intermediate water, *J. Geophys. Res.*, 102, 893-909, 1997.

Yoshida O., Inoue H. Y., Watanabe, S., Noriki S., and Wakatsuchi M, Methane in the western part of the Sea of Okhotsk in 1998-2000. *J. Geophys. Res.*, 109, C09S12, 2004, doi:10.1029/ 2003JC001910.

要　　約

メタン（CH$_4$）は，二酸化炭素や一酸化二窒素と同様に温室効果気体であり，大気中濃度は産業革命以前の700 ppbv から 1000 ppbv 以上増加した。全球的なメタンの収支を理解するためには供給源の定量化が必要であるが，供給源や除去源の見積りには大きな不確実性が残されているのが現状である。

大気中メタンに対する海洋の供給源としての役割は小さいと考えられているが，その度合いは全自然供給源の0.005－3％と見積値に大きな差異があり，より詳細に観測する必要がある。海洋からのメタンの逃散量は，外洋表面水のメタン濃度から主に見積もられてきたが，外洋表面水は大気中メタンに対してわずかに過飽和であるに過ぎない。一方大陸棚を含む沿岸域ではかなりの程度の過飽和が報告されている。たとえ沿岸域の面積が外洋の面積の10分の1しかなくても，過飽和の程度が10倍高ければ有意な量となり得る。しかしながら，メタンの逃散量を詳細に決定するほど沿岸域における観測は行われていない。

オホーツク海は広大な大陸棚を有する縁辺海の1つであり，メタンの過飽和度が高いことによって，大気中メタンに対する重要な供給源となる。

　　熱分解起源のメタンが堆積物から多く染み出していると考えられているが，時空間的に詳細な観測はほとんど行われてこなかった。そこで，夏季オホーツク海西部においてメタンの分布や変動，大気への逃散量を見積もるためにメタン濃度を測定した。サハリン東岸の大陸棚斜面底層（約 200 m）において極めて高い濃度のメタンを観測した。アムール川河川水流入による表層の成層化によって，陸棚上では亜表層における高濃度メタンは表層〜大気へ運ばれていないことがわかった。しかしサハリン東岸の海底が 100 m 以下と浅く岸に近い海域では潮汐による鉛直混合が活発で表層水のメタン濃度も高くなっていた。陸棚斜面で観測された極めて高濃度のメタンは，東サハリン海流の密度 $26.6-26.8$ σ_θ 面に存在しており，岸に沿った南下流や岸からそれて東に向う流れをメタン濃度で追うことが可能であることが示唆された。サハリン北東岸におけるメタンフラックスは最大で 8.6 mol CH_4 km^{-2} d^{-1} と見積もられた。オホーツク海全体の約 55％に相当する夏季オホーツク海西部（0.78×10^6 km^2）からのメタンの逃散量は 0.014 Tg CH_4 y^{-1} と見積もられた。

　　一方外洋では亜表層にメタンの極大が存在することが知られている。水柱でのメタン生成は還元環境下においてメタン生成バクテリアのみによる。ゆえに沈降する有機物粒子や動物プランクトンの消化管内の微小な還元環境でメタンが生成していることになる。そこで解氷時に生物生産が高くなることで知られている南大洋においてメタンの詳細な動態を把握するためにメタン濃度を測定した。南大洋では表層約 200 m でメタン濃度が最も高く，深度を増すにしたがって急激に濃度が減少した。高緯度海域における表層 100 m で最も濃度が高く，飽和度も $106-139$％と高かった。高濃度メタンが観測された高緯度海域においては，植物プランクトンの指標として知られているクロロフィル a とメタン濃度との相関が極めて高く（$R^2 \geqq 0.7$），植物プランクトン−動物プランクトンを介した生物起源メタンが水柱で生成されていると考えられる。また夏季南大洋におけるメタンの逃散量は $1.2-4.0$ mol CH_4 km^{-2} d^{-1} と見積もられ，動物プランクトンが主な供給源となっている海域としては極めて高い値であることが観測された。